TURUN YLIOPISTON JULKAISUJA
ANNALES UNIVERSITATIS TURKUENSIS

SARJA – SER. D OSA – TOM. 1046
MEDICA – ODONTOLOGICA

REPAIR OF SEGMENTAL BONE DEFECTS WITH FIBER-REINFORCED COMPOSITE:
a study of material development and an animal model on rabbits

by

Mikko Hautamäki

TURUN YLIOPISTO
UNIVERSITY OF TURKU

Turku 2012

From the Department of Biomaterials Science, Faculty of Medicine, University of Turku and
Department of Orthopaedics and Traumatology, Turku University Hospital

Supervised by

Professor Pekka Vallittu
Department of Biomaterials Science
Institute of Dentistry
University of Turku
Turku, Finland

Adjunct professor Mervi Puska
Department of Biomaterials Science
Institute of Dentistry
University of Turku
Turku, Finland

Professor Emeritus Allan Aho
Department of Orthopaedics and Traumatology,
Turku University Hospital and University of Turku
Turku, Finland

Reviewed by

Professor Nils R. Gjerdet
Faculty of Medicine and Dentistry, Biomaterials
University of Bergen
Bergen, Norway

And

Professor Reijo Lappalainen
Biomaterials Technology,
Department of Applied Physics, SIB Labs Infrastructure Unit
University of Eastern Finland
Kuopio, Finland

Dissertation Opponent

Professor Jari Salo
Department of Orthopaedics and Traumatology,
Kuopio University Hospital
University of Eastern Finland
Kuopio, Finland

ISBN 978-951-29-5236-6 (PRINT)
ISBN 978-951-29-5237-3 (PDF)
ISSN 0355-9483

Painosalama Oy – Turku, Finland 2012

To my family ….

ABSTRACT

Mikko Hautamäki. **Repair of segmental bone defects with fiber-reinforced composite: a study of material development and an animal model on rabbits**

Department of Biomaterials Science, Institute of Dentistry, Faculty of Medicine, University of Turku and Department of Orthopaedics and Traumatology, Turku University Hospital

Annales Universitas Turkuensis, Turku, Finland, 2012

The Repair of segmental defects in load-bearing long bones is a challenging task because of the diversity of the load affecting the area; axial, bending, shearing and torsional forces all come together to test the stability/ integrity of the bone. The natural biomechanical requirements for bone restorative materials include strength to withstand heavy loads, and adaptivity to conform into a biological environment without disturbing or damaging it. Fiber-reinforced composite (FRC) materials have shown promise, as metals and ceramics have been too rigid, and polymers alone are lacking in strength which is needed for restoration. The versatility of the fiber-reinforced composites also allows tailoring of the composite to meet the multitude of bone properties in the skeleton.

The attachment and incorporation of a bone substitute to bone has been advanced by different surface modification methods. Most often this is achieved by the creation of surface texture, which allows bone growth, onto the substitute, creating a mechanical interlocking. Another method is to alter the chemical properties of the surface to create bonding with the bone – for example with a hydroxyapatite (HA) or a bioactive glass (BG) coating.

A novel fiber-reinforced composite implant material with a porous surface was developed for bone substitution purposes in load-bearing applications. The material's biomechanical properties were tailored with unidirectional fiber reinforcement to match the strength of cortical bone. To advance bone growth onto the material, an optimal surface porosity was created by a dissolution process, and an addition of bioactive glass to the material was explored. The effects of dissolution and orientation of the fiber reinforcement were also evaluated for bone-bonding purposes. The Biological response to the implant material was evaluated in a cell culture study to assure the safety of the materials combined. To test the material's properties in a clinical setting, an animal model was used. A critical-size bone defect in a rabbit's tibia was used to test the material in a load-bearing application, with short- and long-term follow-up, and a histological evaluation of the incorporation to the host bone.

The biomechanical results of the study showed that the material is durable and the tailoring of the properties can be reproduced reliably. The Biological response - ex vivo - to the created surface structure favours the attachment and growth of bone cells, with the additional benefit of bioactive glass appearing on the surface. No toxic reactions to possible agents leaching from the material could be detected in the cell culture study when compared to a nontoxic control material. The mechanical interlocking was enhanced - as expected - with the porosity, whereas the reinforcing fibers protruding from the surface of the implant gave additional strength when tested in a bone-bonding model. Animal experiments verified that the material is capable of withstanding load-bearing conditions in prolonged use without breaking of the material or creating stress shielding effects to the host bone. A Histological examination verified the enhanced incorporation to host bone with an abundance of bone growth onto and over the material. This was achieved with minimal tissue reactions to a foreign body.

An FRC implant with surface porosity displays potential in the field of reconstructive surgery, especially regarding large bone defects with high demands on strength and shape retention in load-bearing areas or flat bones such as facial / cranial bones. The benefits of modifying the strength of the material and adjusting the surface properties with fiber reinforcement and bone-bonding additives to meet the requirements of different bone qualities are still to be fully discovered.

Keywords: fiber-reinforced composite, bone replacement, segmental bone defect, surface porosity, bone bonding, PMMA, polymethyl methacrylate, bioactive glass

TIIVISTELMÄ

Mikko Hautamäki. **Kuitulujitteinen muovikomposiittimateriaali luunkorvikkeena – materiaalikehitys ja koe-eläintyö luun segmenttidefektimallilla**

Biomateriaalitieteen oppiaine, Hammaslääketieteen laitos, Turun Yliopisto ja Ortopedian ja Traumatologian klinikka, TYKS,
Annales Universitas Turkuensis, Turku, Suomi, 2012

Segmentaalisten luupuutosten korvaaminen painoa kantavien putkiluiden osalta on vaativa tehtävä, koska niihin kohdistuu monenlaista rasitusta: luun pituusakselin suuntaista (puristava ja vetävä), taivuttavaa sekä kiertävää. Luunkorvikemateriaalin tulee olla riittävän kestävä kyetäkseen vastaanottamaan siihen kohdistuvan luonnollisen rasituksen, mutta lisäksi sen tulee olla joustava sulautuakseen osaksi luonnollista luista ympäristöä, häiritsemättä sen toimintaa. Metalli-implantit ja keraamit ovat kovia ja kestäviä materiaaleja ja soveltuvat käytettäväksi luunkorvikkeina, mutta niiden luontainen jäykkyys aiheuttaa rasituksen lisääntymistä raja-alueilla. Polymeerit yksinään ovat usein liian heikkoja mekaanisilta ominaisuuksiltaan käytettäväksi luunkorvikkeina. Kuitulujitteiset polymeerit ovat osoittaneet omaavansa vaadittavan mekaanisen lujuuden, ja mahdollistavansa myös lujuusominaisuuksien muuntelun vastaamaan kohdekudoksen asettamia vaatimuksia.

Luunkorvikemateriaalien kiinnittymistä luuhun on pyritty lisäämään muuntamalla materiaalin pinnan ominaisuuksia monin eri keinoin. Yleisimmin käytetty menetelmä on materiaalin pinnan tekeminen epätasaiseksi (karhentaminen tai huokoistaminen) kasvattamaan mekaanisen kiinnityksen mahdollistavaa pinta-alaa. Toinen vaihtoehto on muokata pinnan kemiallisia ominaisuuksia– esimerkiksi hydroksiapatiitti (HA-) tai biolasi (BG-) pinnoituksella – lisäämään luun kasvua kiinni suoraan materiaalin pintaan.

Tutkimuksen aikana kehitettiin kuitulujitteinen muovikomposiitti (FRC), jolla on huokoistettu pintarakenne. Implantin lujuusominaisuudet muokattiin vastaamaan kortikaaliluun biomekaanisia ominaisuuksia käyttämällä pitkittäistä yhdensuuntaista kuitulujitusta, mahdollistaen sen käytön painoa kantavissa rakenteissa. Materiaalin pinta tehtiin huokoiseksi erityisellä liuotus-/vaahdotus menetelmällä, joka muodosti avoimen huokosrakenteen, johon luu voi kasvaa sisälle. Vaahdotusprosessissa tutkittiin mahdollisuutta kiinnittää pintaan bioaktiivista lasia rakeina lisäämään luun kasvua materiaaliin. Liuotusmenetelmän ja kuitulujituksen vaikutuksia pinnan huokoisuuteen sekä luun kiinnittymiseen tähän pintaan testattiin erillisessä työssä. Soluviljelykokeessa testattiin kehitetyn materiaalin turvallisuutta sekä tarkasteltiin pinnan ominaisuuksien vaikutusta solujen kasvuun. Koe-eläinmallilla testattiin kehitetyn luunkorvikemateriaalin toimivuutta kantavan rakenteen – kanin sääriluun segmenttidefekti - korjaamiseen, sekä eläimen elimistön vastetta käytetylle materiaalille.

Biomekaaniset tulokset osoittivat materiaalin omaavan vaadittavat ominaisuudet kestääkseen kantavissa luurakenteissa, ja että materiaalin valmistusprosessi oli toistettavissa luotettavasti. Soluviljelukokeissa ei ilmennyt haitallisia reaktioita kehitettyä materiaalia kohtaan, ja pinnan karhennus sekä bioaktiivinen lasi lisäsivät solujen kasvua materiaalin pinnalla. Materiaalin pinnan huokoistus jo yksinään kasvatti koekappaleiden kiinnittymisen lujuutta, mutta liuotusprosessin paljastamat kuidut lisäsivät kiinnittymistä. Eläinkokeissa materiaali osoittautui kestävän siihen kohdistuneen painorasituksen ilman koekappaleiden hajoamista tai merkittävää luun resorptiota. Histologinen tarkastelu osoitti materiaalin mahdollistavan luun kasvun materiaalin pintaa pitkin ja pinnan huokoistuksen sisään, ilman merkittäviä kudoksen vierasesinereaktioita.

Kuitulujitteinen muovikomposiitti-implantti on jo osoittanut hyviä tuloksia korvattaessa luupuutoksia vaativissa rakenteissa kuten litteiden luiden korvaamisessa kasvo – ja kalloluiden alueella koe-henkilöillä, sekä kantavissa rakenteissa koe-eläinmalleissa. Materiaalin etuina ovat monipuoliset mahdollisuudet materiaalin lujuuden ja pintaominaisuuksien muokkaamiseen. Materiaalin hyvät työstöominaisuudet mahdollistavat jatkossa kehityksen aina perusmuotoisista massaimplanteista jopa yksilöllisesti valmistettaviin kolmiulotteisiin implantteihin.

Avainsanat: kuitulujitus, muovikomposiitti, luun korvikemateriaali, luupuutos, polymetylmetakrylaatti, pintahuokoisuus, luun kiinnittyminen

TABLE OF CONTENTS

LIST OF ORIGINAL PUBLICATIONS

This thesis is based on the following original articles that are referred to in the text by the Roman numerals I-IV.

I **Aho AJ, Hautamäki M, Mattila R, Alander P, Strandberg N, Rekola J, Gunn J, Lassila LV, Vallittu PK.** Surface porous fibre-reinforced composite bulk bone substitute. Cell and Tissue Banking 2004;5(4):213-21.

II **Hautamäki M, Aho AJ, Alander P, Rekola J, Gunn J, Strandberg N, Vallittu PK** Repair of bone segment defects with surface porous fiber‐reinforced polymethyl methacrylate (PMMA) composite prosthesis: Histomorphometric incorporation model and characterization by SEM. Acta Orthopaedica 2008, Vol. 79, No. 4 , Pages 555-564

III **Hautamäki M, Meretoja VV, Mattila RH, Aho AJ, Vallittu PK**. Osteoblast response to polymethyl methacrylate bioactive glass composite. Journal of Material Science: Materials in Medicine. 2010;21(5):1685-92.

IV **Hautamäki MP, Puska MA, Kopperud HM, Aho AJ, Vallittu PK** Surface structure of fiber-reinforced composite implant and its effect on the attachment of implant to simulating bone material – Submitted

Thesis contains also previously unpublished results. Reproduction of original articles is made by permission of the copyright holders.

List of abbreviations

MMA	methyl methacrylate
PMMA	polymethyl methacrylate
FRC	fiber-reinforced composite
THF	tetrahydrofuran
E-glass	electrical grade glass
HA	hydroxyapatite
BG	bioactive glass
MPa	megapascal
GPa	gigapascal
M_w	molecular weight
BCI	bone contact index
SEM	scanning electron microscope
RNA	ribonucleic acid
PCR	polymerase chain reaction
BSP	bone sialoprotein
OC	Osteocalcin
$CaSO_4$	calcium sulphate
$CaCO_3$	calcium carbonate
TCP	tricalcium phosphate
GIC	glass ionomer cements
BisGMA	bisphenol-A-glycidyl dimethacrylate
TEGDMA	Triethylene glycol mimethacrylate
TGF	transforming growth factor
IGF	insulin-like growth factor
BMP	bone morphogenetic protein
IL	interleukin
TNF	tumor necrosis factor
MMP	matrix metalloproteinase
TGF-β	transforming growth factor-β
FGF	fibroblast growth factor
RANKL	receptor activator of nuclear factor kappa-B ligand
VEGF	vascular endothelial growth factor
PDGF	platelet-derived growth factor
PGA	polyglycolic acid
PLLA	polylactid acid
PCL	polycaprolactone
PE	polyethene
UHMWPE	ultra-high molecular-weight polyeth(yl)ene
PP	polypropylene
PTFE	polytetrafluoroethylene
PVC	polyvinyl chloride
PC	polycarbonate
PET	polyethylene terephthalate
PEEK	polyether-etherketone
PSU	polysulfone
Porogen	pore-forming agent, an additive

1. INTRODUCTION

The Repair of bone defects has been studied experimentally since the age of the Pharaohs when scull defects after trepanations were replaced with metal, gold, or ivory patches. Despite the advances in medicine, large bone defects in load-bearing areas still present a problem for the medical professionals of the modern day. Currently, a missing bone is most often replaced with massive bone allograft transplants, harvested from donors, or with metallic implants. Both of these methods have their own drawbacks that interfere with the short- and long-term results. (Bobyn et al. 1999, Shin et al. 2000, Tanzer et al. 2003)

Large structural allografts possess biological features such as natural bone mineral (hydroxyl apatite) and proteins (collagen fibers, bone morphogenetic proteins, etc.) to aid in the incorporation of the transplanted bone. Still, the process of incorporation is slow and often incomplete, and can lead to undesired resorption or rejection reactions, not to mention a transport of possible infectious agents to the host (Aho et al. 1998, Zimmermann and Moghaddam 2011).

Metallic implants are capable of withstanding the load applied to them, but the rigidity can cause the host bone to deteriorate around it and the implant becomes loosened over time. (Shin 2000, Lindahl et al. 2005) Different approaches to enhance the adhesion of metallic implants have been tested in the last decades, especially in the field of joint replacement surgery. Rough surface topography and different coating methods have improved the success rate of many joint prosthetic devices, but the difficulty of maintaining adhesion and incorporation to host bone still exists. (Brown and Ring 1985, Bobyn et al. 1999, Hacking et al. 2003, Hallan et al. 2007)

Biomaterial composites have become a viable alternative to metallic implants in the recent years. They provide a multitude of options for vascular grafts and stents, the fixation of fractures, the attachment of tendons and even replacing small bone defects. They are of special interest because of their reduced weight, radiolucency and lower stiffness when compared to metals (Gasser 2000). Furthermore, the polymer composites do not cause interference or special safety precautions related to metal implants when using modern diagnostic tools such as CT or MRI (Sawyer-Glover and Shellock 2000, Shellock 2002). New methods of fiber reinforcement have increased the strength and durability of conventional polymer materials so that they can be used as bone substitutes (Vallittu 1999, Tuusa et al. 2007, Mattila et al. 2009, Ballo et al. 2009)

As metallic implants have been found to be too rigid, ceramic implants too fragile and pure polymer implants too weak to be used as succesfull bone replacement materials in load-bearing surroundings, the fiber-reinforced composites (FRCs) present an interesting alternative. The strength and stiffness of an FRC can be changed by altering the type and amount of reinforcing fibers added into the composite matrix. This allows customizing of the biomechanical and surface properties of the FRC to meet the requirements of a specific area of the skeleton. The subject of the present thesis was to investigate a novel (FRC) material to be used for bone replacement purposes. The biomechanical properties of the material were developed aiming for the properties of human bone, and were compared to conventional polymethyl methacrylate (PMMA) cement properties (study I). A method to fabricate a porous surface stucture onto the implant was evaluated with a scanning electron microscope (SEM), and the effect of the surface porosity in increasing the bone bonding was analyzed (studies I,II and IV). The Safety of the new FRC material was tested in vitro by the use of osteoblast cell cultures, where the normal cellular functions were assessed by soluble markers,and SEM imaging (study III). The functioning of the FRC implant as a segment defect replacement material was tested in an animal model. The animal model of a large segmental defect in a long bone and load-bearing application was used to test the FRC implant. The durability of the implant, the host's responses to the material, and the incorporation of the implant to the host bone were evaluated from histological samples gathered from the animals (studies I and II).

2. REVIEW OF THE LITERATURE

2.1. – Bone

Bone is a strong specialized connective tissue, which enables mammals to move with the aid of the muscles attached to the bones, and also gives shelter and support to their bodies' vital organs such as the brain, lungs, liver, etc. Bones also act as a storage for ions (Ca-, PO_4-, Na-, Mg-, etc) that regulate many cellular functions, and they harbor pluripotent stem cells in the bone marrow to enable the growth of new cells essential to support life.

2.1.1. Genesis

Connective tissue, cartilage, and bone differentiate from the diffuse mesoderm known as mesenchyme. The mesenchyme emerges mainly from the primitive streak and secondarily from mesodermal segments and the lateral somatic and splanchnic layers of the mesoderm. Bone tissue is formed during fetal mesenchymal development by two mechanisms: intramembranous and endochondral. Intramembranous formation occurs when the mesenchymal cells cluster together, transform to osteoblasts and then to osteocytes, as they begin to secrete mineralized extracellular matrix around them (osteoid), forming bone. In endochondral ossification, the mesenchymal cells also condense and proliferate, but instead of turning into osteoblasts, they become chondroblasts and secrete extracellular matrix pilkku forming a cartillaginous model of a bone. Blood vessels infiltrate this matrix, and it begins to deteriorate as the chondrocytes die and osteoblasts, carried by the blood vessels, begin to secrete the bone matrix, finally replacing all of the cartillage. This development continues even in adolescent mammals, as the longitudinal growth which happens in the epiphyseal plates (growth plates) of bones is endochondral. The Majority of bones are formed through endochondral formation, with the exception of the flat bones of the skull, the diaphyses of long bones and the clavicle. (Dietz and Morcuende, 2006)

2.1.2. Structure and biomechanics

Bone is a tissue in which living cells make up only 2 to 5% of the volume. Although water in its free form is not found in bone as it is in other connective tissue, 10 % of the weight of bone is comprised of water in other forms . The rest is non-living material which comprises 95 to 98%. This non-living material surrounding the cells - also called the osteoid - is mainly made of a mineral-encrusted protein matrix, with the mineral (compostition of calcium phospahtes, -carbonates and -sitrates) comprising about half of the volume, but 60 % of the weight of the bone. The organic matrix – which makes up about 30% of the weight of the bone - is primarily collagenous (type I collagen - 95%), and the rest of the proteins include many noncollagenous proteins such as glycosaminoglycans, osteonectin, fibronectin, matrix gla-protein, osteopontin, bone sialoprotein and growth factors.

The bone has many levels and structures: the macrostructure (cancellous and cortical bone), the microstructure (Haversian systems, osteons, single trabeculae), the sub-microstructure (lamellae), the nanostructure (fibrillar collagen and embedded mineral), the sub-nanostructure (below a few hundred nanometers), molecular structure of constituent elements, such as mineral, collagen, and non-collagenous organic proteins. (Aho 1966, Rho 1998) This is illustrated in Figure 2.1. A long bone – typically the bones of the limbs – consists of end segments called caput (or epiphyses), a tubular shaft which is called a diaphysis, and the flared portion of the shaft merging with the region of the growth plate and the caput, which is called a metaphysis. Figure 2.2 presents a structure of a long bone (femur).

Bone is a biological fiber-reinforced composite and it can be compared to steel-reinforced concrete or fiber-reinforced plastic, where the porous concrete/plastic equals mineralised calcium salts, and steel rods/fibers equal collagen fibers. It is also capable of adapting to the stress applied to it – remodeling often referred to as Wolff's law – by optimizing the weight-to-strength ratio (Pearson and Lieberman 2004). Bone can increase its strength in a number of ways: by increasing bone mass (trabeculae in cancellous bone), by changing the bone geometry (enlarge radius of cortical bone) to redistribute the forces that it must resist, or by alterations oto its microstructure (Haversian canal system). (Pearson and Lieberman 2004, Heaney 2006, Barak et al. 2011)

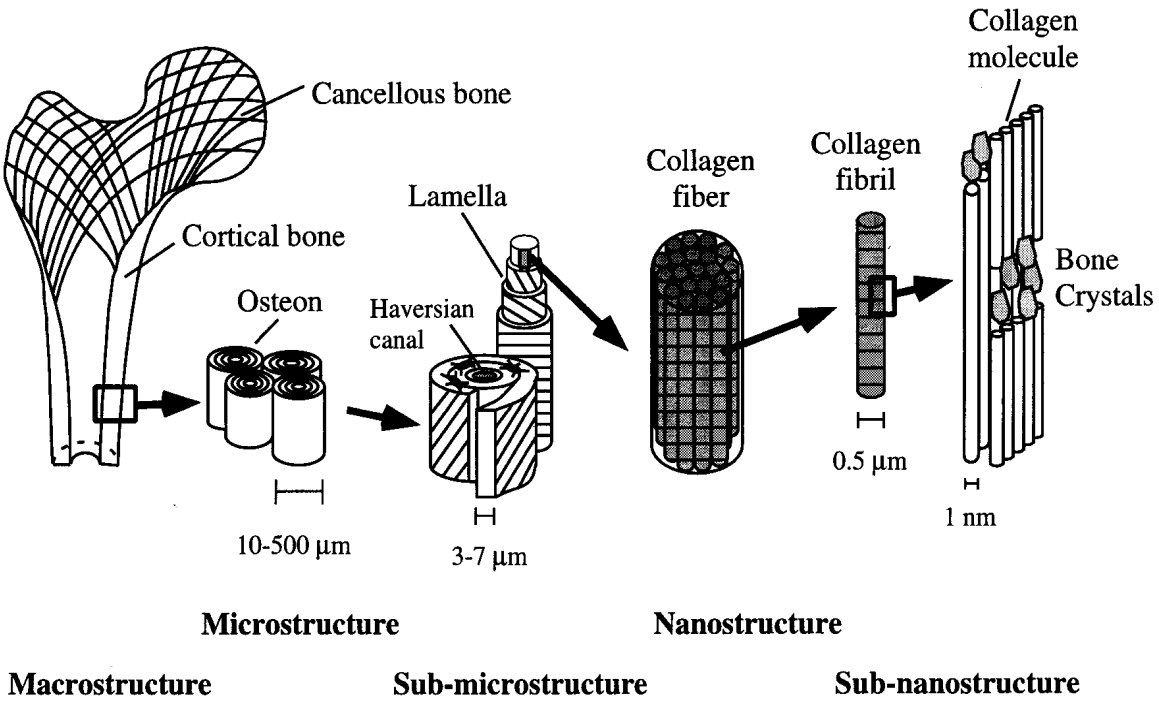

Figure 2.1 – An illustration of the structure of bone – adapted from Rho et al. (1998)

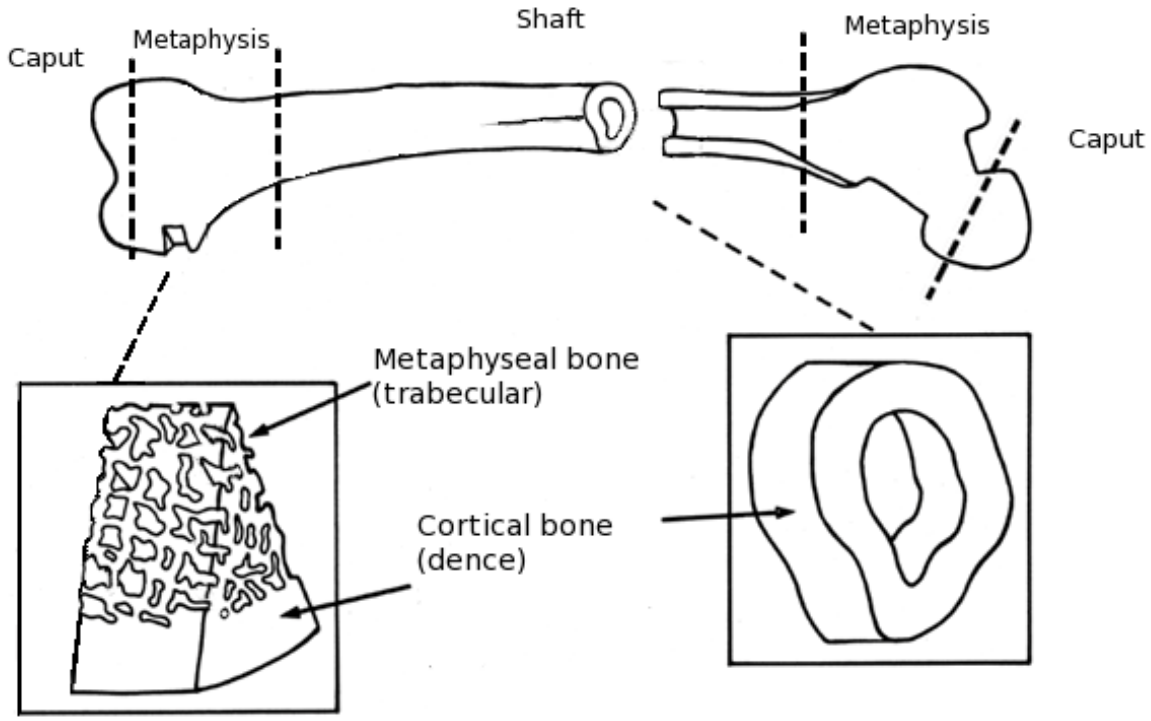

Figure 2. 2 – Structure of a long bone

As bone is capable of reacting to increased stress, it also alters its form according to reduced stress by decreasing the total mass of bone mineral. This can be seen in osteoporosis (age-, immobilization- or medically induced), where the thickness of the cortex and the density of the trabecular bone are reduced. The same phenomena is witnessed around stiff metal implants (high elastic modulus) such as total hip replacement stems, bone tumor prostheses, knee prostheses and fracture repair devices (angle-stable plates). This event is known as stress shielding effect which is caused by the difference in the mechanical properties (stiffness) of bone and metal implants. The bone is less strained because the implant supports the weight (above and near the implant) more than the bone. This causes resorption of the bone - in areas where little strain is applied to the bone - not simply due to bone damage, but rather caused by the redistribution of stress along the bone. This difference in mechanical properties of bone and bone implant can lead to aseptic loosening of the implants or fractures in the weakened bone under normal stress. (Engh et al. 1987, Huiskes 1992, van Lenthe et al. 1997, Shin 2000, Keaveny et al. 2001, Lindahl et al. 2005, Sundfeld et al. 2006, Ulstrup 2008)
Determining the exact mechanical values of bone is difficult, since the properties vary greatly according to the anatomical location within the bone (caput, metaphysis, shaft). Bone is an anisotropic material as its properties differ according to the direction in which the specimen is tested (longitudinal to transverse or compression to tension). Longitudinal compressive forces are tolerated best, as the bone tissue is accommodated to resisting forces (gravity) in a longitunal direction, intermediately in tension and least in transverse way (shear/rotational). In addition age, diseases, the mineral content, the purpose of the bone (patella - bone in tendon vs long bone), and possible prior damage/repairs to the bone affect the results. The average biomechanical values of human bone are gathered in Table 2.1., altough they vary substantially between different sources. (Lotz et al. 1991, Rho et al. 1997, Morgan and Keaveny 2001, Bayraktar et al. 2004)

The Biomechanical properties of bone differ greatly depending on the purpose and location of the bone. Metaphyseal areas, the majority of the carpal bones of the hand, the bones of the foot (talus, calcaneus, cuboideum, navicular, cuneiforms) and the corpus of the vertebrae consist mainly of cancellous (trabecular) bone, which is weak in biomechanical properties, but has a large surface area and a high metabolic activity. The trabecular bone possesses a capability to ”flex” under great stress, by allowing microstructural damage to dissipate energy which otherwise could damage the bone’s macro structure (creating a fracture). A large part of the bone marrow also resides in metaphyseal bone. Cortical (dense) bone is responsible for the structural support of the skeleton as its compressive and tensile strength surpasses any other tissue in the body. Even though cortical bone is strong, it is also flexible as it can withstand deformation to certain extent without breaking (fracture). Force (stress) applied to a bone creates deformation (strain), which is elastic until yield point is reached. The slope of the stress /strain curve retrieved from biomechanical testing of a bone corresponds to the elastic modulus of the bone. (Figure 2.3) An elastic deformation is capable of returning to its normal state as before the force was applied. If force is applied over the yield point, a plastic deformation occurs and this deformation does not entirely return to its original state. Bone rapidly loses its capability to withstand plastic deformation and the bone ‘s structure is damaged, when the ultimate strength is exeeded. A plastic deformation has also been shown to develop into fractures (stress fractures) with sub-yield stress applied repeatedly (cyclic loading), or with constant near yield-point forces. (Rho et al.1997, Reilly and Currey 1999, Keaveny et al. 2001, Morgan and Keaveny 2001,Turner 2006, Burr 2011).

Table 2.1 Properties of human bone (according to Rho 1997, Lotz et al. 1991, Bayraktar et al. 2004)

	Elastic modulus (GPa)	Compressive (MPa)	Tension (MPa)
Cortical bone	12.5 -25.9	614-736	107.9
Trabecular bone	3.5 -18.7	135	84.9

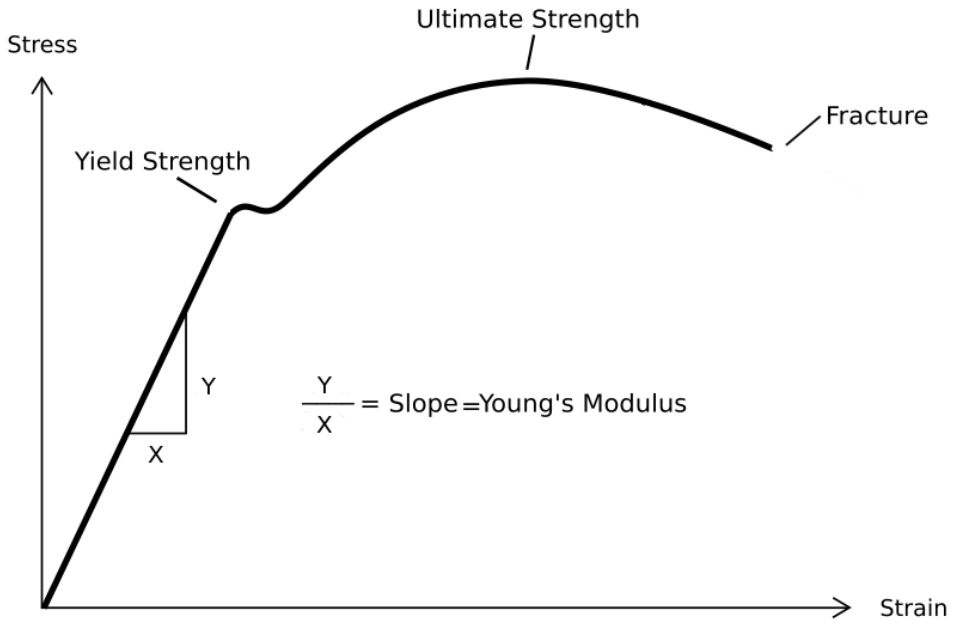

Figure 2.3 Force vs the Displacement curve of bone

2.1.3. Damage and repair

Bone breaks rather easily, as only about 15 joules (J) of energy is needed to break the shaft of an adult tibia or femur. A person, weighing 70 kilograms, falling from a standing position, produces 500 joules of energy", whereupon much of the energy has to be absorbed by the soft tissues and muscles to prevent bones from breaking. In addition, the structure and orientation of lamellae and osteons of bone guide the forces so that a maximum amount of energy is absorbed in circular or longitudinal smaller cracks of the fracture with minimal damage to the whole structure. If such a total damage (fracture) occurs, bone is generally able to repair itself through a healing process, and due to its remodeling properties, with minimal residual scar formation.

A fracture initiates a biologic cascade - as steps are activated by and depending on the previous steps - which is considered to involve three main phases: inflammatory, reparative and remodeling. Many subsections can be identified in each step, and most of them are overlapping because the repair is at different stages in different parts of the fracture. When a fracture ruptures the periosteum and Haversian canals, it injures the blood vessels, causing bleeding. This creates a haematoma and local bone necrosis, and the tissue is invaded by polymorphonuclear leucocytes, macrophages and mononuclear cells, beginning the inflammatory phase of bone repair. The inflammatory cells secrete cytokines (IL-1, IL-2, RANKL, TNF x, TNF b). The healing cascade induces the production of growth factors (bone morphogenetic proteins (BMPs), matrix metalloproteinases (MMPs), transforming growth factors (TGF-β), fibroblast growth factors (FGF1, 2), angiogenic growth factors (VEGF a→d), platelet-derived growth factor (PDGF), etc.) to promote the differentiation of fibroblasts and osteoblasts, and the growth and invasion of blood vessels. The cells needed for the repair are recruited from the hematoma, Haversian canals, bone marrow and surrounding periosteum. Bone repair (reparative phase) begins when chondrocytes activate within the hematoma at the fracture site, and woven bone is laid down with the formation of a provisional fibrocartilaginous callus. Moreover, the osteocytes within the periosteum - several centimeters away from the fracture site – activate and begin forming new woven bone that finally grows over the fracture site. This weak woven bone acts as a template for the stronger lamellar bone, which is deposited onto it by activated osteoblasts. The remodeling phase of the repair continues long after the bone has regained its previous strength, as the bone adapts to the strain presented to it. (Madison and Martin 2001, Al-Aql et al. 2008, Shapiro 2008, Ulstrup 2008)

In histology, the healing of fractures has classically been divided into direct (primary) and indirect (secondary) fracture healing. Four basic new bone formation processes occur during fracture repair: osteochondral ossification, intramembranous ossification, oppositional new bone formation, osteonal migration (creeping substitution). Direct or primary cortical fracture healing occurs only when there is

anatomic reduction of the fracture fragments by rigid fixation. The process involves an attempt to re-establish the Haversian systems by discrete remodeling. During this process, only a little or no periosteal response is noted (no callus formation). Indirect or secondary fracture healing involves a combination of intramembranous and endochondral ossification - as in the fetal bone development - with the subsequent formation of a callus. Motion between the fragments leads to secondry healing.

Intramembranous ossification involves the formation of bone directly - without first forming cartilage - from mesenchymal cells that reside in the periosteum. The resulting callus can be described histologically as a “hard callus”. In endochondral ossification, the mesenchymal cells form into cartilage which becomes calcified and eventually replaced by bone. Its temporal characteristics include six identifiable stages: haematoma formation and inflammation, angiogenesis and cartilage formation, calcification of cartilage, cartilage removal, formation of bone, and finally, bone remodeling. This type of fracture healing - stabilizing through periosteum and the external soft tissues - provides an early bridging callus, histologically described as a “soft callus”. (Chao et al. 1998, Madison and Martin 2001, Dimitriou et al. 2005)

The aforementioned healing patterns can be expected when the ends of the bone are in a close proximity to each other and the periosteum is present. When there are defects in the bone with a long gap between the ends of the bone (after tumor surgery, trauma or infection) or the other end is missing (amputated limbs), the repair pattern is altered. As the the periosteum is missing along with the osteoprogenitor cells, and the bone marrow alone is not capable of propagating the healing, the ends of the bone become rounded and the soft tissue invades the gap, creating a non-union, even if the bone is stabilized internally or externally. These critical-sized defects - “a defect that will not heal spontaneously during the lifetime of the animal” – have been defined as segmental defects with a length exceeding 2-2.5 times the diameter of the affected bone. (Bruder et al. 1998, Teixeira and Urist 1998, Reichert et al. 2009, Tiemann et al. 2009)

2.2. Bone grafting for segmental defects

2.2.1 Bone grafts

An ideal bone graft material should exhibit many properties which include the ability to chemically bond to the surface of bone without an intervening layer of fibrous tissue (osteointegration), the ability to support the growth of bone over its surface (osteoconduction), the ability to induce differentiation of pluripotential stem cells from the surrounding tissue to an osteoblastic phenotype (osteoinduction), and the formation of new bone by osteoblastic cells present within the graft material (osteogenesis). (Einhorn 1995, Moore et al. 2001)

Autogenous bone – bone taken from the host itself – possesses all of these properties and is still considered the golden standard of bone grafting. Autogenous bone can be harvested as a cancellous (trabecular /metaphyseal) graft from the iliac crests or the metaphyses of long bones, or as a cortico-cancellous bone graft from the iliac crest, fibula or ribs. The cancellous bone is known to revascularize rapidly and promote the healing of non-united or infected fractures, and is capable of spanning gaps up to 4 cm in length in favorable circumstances. All of the autografts are of limited quantity, and only fibular grafts possess the structural integrity to succeed in weight-bearing areas replacing segmental defects. The success of the free cortical (non-vascularized) grafts is complicated by the slow and often incomplete revascularization, and poor incorporation as the healing happens through creeping substitution. Both of these can result in a delayed union, a non-union, a resorbtion or a fracture of the graft. (Enneking et al. 1980, Tiemann et al. 2009, Eward et al. 2010) A vascularized bone graft can overcome some of these problems, but it is technically demanding and still subject to a long remodeling time and a high fracture rate. (Paley and Maar 2000, Mekhail et al. 2004, Nishida and Shimamura 2008)

Viable options to repair large segmental defects also include bone transport and bone lengthening by external (Ilizarow or Taylor Spatial frame) or internal (lengthening intramedullary nail) devices. Both of these methods rely on the continuous creation of new bone between the slow-moving ends of the bone. The advantages of these methods include minimal soft tissue trauma, the fact that large bone defects can be treated with the same bone diameter, a gradual correction of deformities, and a limited donor-site morbidity. The drawbacks include liability to (superficial and deep) infections, a long treatment time, stiffness of adjoining joints, non-unions and a dependence on patient compliance. (Paley

and Maar 2000, Mekhail et al. 2004)

An Allogenous bone graft – taken from a human donor – or a xenogenous bone graft – taken from another animal species – can also be used after proper processing as segmental bone grafts. Depending on the processing method (washing, freezing, demineralization, decellularization, heat treatment/ sintering etc.), these grafts possess variable osteoinductive (releasing bone morphogenic proteins) and osteoconductive properties, but they all lack viable cells and thus osteogenic potential. Despite all the advancements in the preparation processes, there is still the possibility of a disease (HIV, HCV, bacterial, prions) transmission from the donor to the recipient. The same disadvantages prevail as with cortical autografts: slow vascularization, deficient incorporation and susceptibility to fractures. (Hesse et al. 2010, Zimmerman and Moghaddam 2011)

2.2.2. – Artificial materials as substitutes for segmental defects

Metals: In the replacement of segmental defects, the use of metal is well documented by the use of megaprostheses in tumor surgery. Metals have good biomechanical strength through stiffness, which often causes loosening of the implant through stress shielding effect as the stiffness of metals can be even five to twenty times higher than with cortical bone. (Huiskes et al. 1992, Mittermayer et al. 2002) Solid metal implants lack the flexibility of bone, and also the biological incorporation to bone is limited to minor surface roughness creating the interlocking. These obstacles have been overcome with the use of porous materials (tantalum), TNTZ alloy (Ti–29Nb–13Ta–4.6Zr) (TNTZ) or gages /mesh (titanium) to increase bone ingrowth and the flexibility of the implant with some good results. (Ray et al. 1997, Bobyn et al. 1999, Murakami et al. 2002, Niinomi 2008)

Inorganic Compounds: For over a century, inorganic compounds, like plaster of Paris - calcium sulphate ($CaSO_4$), i.e. Gypsum (reported by Dreesman in 1892) - have been used in the treatment of bone. Since then, a multitude of artificial materials has been presented, but they all rely on the Ca-P-rich layer formation to achieve bone bonding. (Hench 1998, Välimäki and Aro 2005) Some materials originate directly from nature, such as algae (choral), where hydroxyapatite is derived through conversion of calcium carbonate ($CaCO_3$) to calcium phosphate [$(Ca_n(PO_4)_m$]. This choral bone material is similarly porous as bone and well incorporated, but lacks the structural strength. Bone - allogenous or xenogenous - can be processed chemically to create demineralized bone matrix products (paste, granules, blocks) containing the collagenous framework and a part of the osteopromotive protein complexes of bone. Another method of treating bone is through high temperature sintering or chemical decomposition to remove all organic material from the bone to produce hydroxyapatite (HA) [$(Ca_5(PO_4)_3(OH)$]. HA-products have a good biocapatibility and they are osteoconductive, but their incorporation and substitution is minimal at best, rendering the material a space filler. β-tricalsium phosphate [$Ca_3(PO_4)_2$] (TCP) possesses good properties for osteoconduction and can be incorporated to bone well. TCP can be derived synthetically through a high temperature calcination process or by a partial conversion of HA products. New applications of calcium phosphates include combinations with carbonates to form calcium phosphate cements (CPC), which are moldable and injectable, but fast-setting, and once hardened, possess some structural strength. All these materials have shown good compatibility with host bone in experimental and clinical applications, but they are often inferior in mechanical stability, compared to cortical bone. (Frankeburg et al. 1998, Moore et al. 2001, Karaoglu et al. 2002, Finkemeier 2002, Giannoudis et al. 2005, Tadic and Eppley et al. 2005, Zimmermann and Mohaddam 2011)

Scaffolds: Porous ceramic cylinders (usually HA or TCP) with combinations of mesenchymal stem cells, bone marrow aspirate or an addition of osteoinductive growth factors (Transforming Growth Factor (TGF), Insulin-like Growth Factor (IGF), Bone Morphogenetic Proteins (BMP)) have also been studied in an attempt to enhance the bone growth into the implant and to advance incorporation in segmental defects. (Bruder et al. 1998, den Boer et al. 2003, Giannoudis et al. 2005, Reichert et al. 2009) Long bone defect models using a platelet-rich plasma-loaded collagen scaffold have also been studied with controversial results. (Sarkar et al. 2006)

Bioactive glasses (BG): BGs have evoked great interest towards these silica-based ceramics since their introduction in the 1970's by Hench. Bioactive glasses have different compositions, but primarily they are made of SiO_2, Na_2O, CaO, K_2O, MgO, P_2O_5, B_2O_3, and they are produced as granules, fibers and in block form. The composition of the glass affects their bioactivity and also the rate of resorption. The critical feature for bioactivity is the SiO2 content of the glass, and the content of 45–52% (%-w), is considered

the most favorable for rapid bone bonding. The upper limit of SiO_2 content for the material to be resorbable and active varies between sources from 60-%w to 71-%w. The formation of the Si-rich layer in wet surroundings is crucial for bone bonding, as it acts as a template for calcium phosphate precipitation enabling bone bonding. The bioactive glasses have shown to possess several unique properties compared to other synthetic bioresorbable bioactive ceramics - such as calcium phosphates, hydroxyapatite (HA) and tricalcium phosphate (TCP) - as they are capable of direct bone bonding, stimulating the growth and maturation of osteoblasts, and promote the expression and maintenance of the osteoblastic phenotype. (Cao and Hench 1995, Hench 1998, Wheeler et al. 1998, Livingston et al. 2002, Itälä et al. 2003, Välimäki and Aro 2005)

Biodegradable polymers: The bioabsorbable polymers, based primarily on α-hydroxy acids, have been in clinical use for over 40 years, at first as suture material, but later as pins, screws and plates. The most common synthetic absorbable polymers are polyglycolic acid (PGA), polylactic acid (PLLA), polycaprolactone (PCL) and their copolymers, which can all be degraded in the living tissue by hydrolysis and then metabolically digested to water and carbon dioxide (CO_2). Biopolymers themselves have evolved tremendously in stability during the past decades, and especially in strength through the creation of self-reinforcing polymers, but they are still deficient in biomechanical strength for replacing bone defects in weight-bearing areas. Composites of bioactive ceramics (HA, TCP and BG) and resorbable materials have been investigated in attempts to create a material for weight-bearing circumstances (Ignatius et al. 2001, Närhi et al. 2003, Eppley et al. 2005, Giannoudis et al. 2005, Lu et al. 2005, Kolk et al. 2012)

Biostable polymers: Many non-resorbable polymers have been found biocompatible, and some of them - polymethyl methacrylate (PMMA), polyethylene (PE), polypropylene (PP), polyurethane (PU), polytetrafluoroethylene (PTFE), polyamides (PA), polycarbonate (PC), polyethylene terephthalate (PET), polyether-etherketone (PEEK), and polysulfone (PSU) - have been investigated for bone tissue replacement purposes. (Gasser 2000, Ramakrishna et al. 2001, Wang 2003, Fujihara et al. 2004, Wang 2004)
Bone cement (polymethyl methacrylate) $[(C_5O_2H_8)_n]$ has been used as a bone replacement material for defects since its introduction by Charnley (1960) in the 1950's to fixate metal hip replacements to bone. The self-curing PMMA cement is an autopolymerizing material, which can be prepared from monomer of methacrylate and polymer powder of polymethacrylate ex vivo and then inserted as a paste to the recipient site, where it takes the exact shape of the host bone. The polymerized end product is hard and non-soluble, but still capable of some deformation without breaking due to the nature of long polymer chains without cross-linkings. The polymerization process is exothermal, causing tissue damage to the surroundings, and the release of harmful monomers and free radicals during and after the polymerization process has been documented. Different compositions of cements have been introduced over the decades with different bioactive filler materials (GIC, BG), resin additives and cross-linking (BisGMA/ TEGDMA) agents in a quest for better mechanical strength and biocompatibility. The bioactive filler cements have shown promise also in clinical settings, but the cements with resin additives or cross-linking agents have even presented some detrimental effects to surrounding tissues, including rapid loosening and necrosis. (Lewis 1997, Lu et al. 2001, Lucksanasombool et al. 2002, Miyazaki et al. 2003, Puska et al. 2004, Giannoudis et al. 2005, Puska et al. 2005a, Puska et al. 2005 b, Zimmermann and Moghaddam 2011)

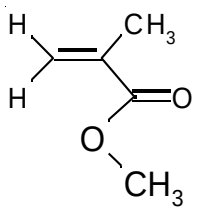

Structure of methyl methacrylate (MMA)

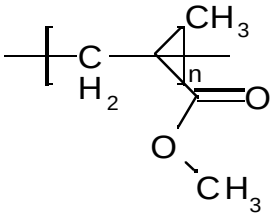

Basic structure of polymethyl methacrylate (PMMA)

2.3. – Fiber-reinforced Composites

Composite materials consist of two or more different material components (phases) which are combined to improve the material's physical, mechanical or biological properties. Nearly all parts of human body can be considered composites: bone, skin, cartilage, dentin, etc. The main component of the composite is called the matrix phase, and in medical use it is generally a biocompatible polymer (bioabsorbable or non-absorbable). The second material is either an additive or a reinforcing material, which can be a polymer, inorganic or metallic by composition. Typically, the matrix has inferior strength in compression and tension, compared to the reinforcement. The reinforcing material can be either in particulate, fiber or laminate form. Theoretically, by increasing the amount of the reinforcing agent, the composite's mechanical properties shift from the matrix's properties towards the properties of the reinforcing material. The mechanical properties (strength and modulus) of a composite are affected by the size, shape, distribution and aspect ratio (volume/mass) of the reinforcing agent, as well as by the strength of the interaction between the matrix and the reinforcement (interface/attachment). As a conclusion, the properties of a composite can be tailored to reach the desired result. (Gasser 2000, Hull and Clyne 2002, Wang 2003)

The simplest way to approach a composite's theoretical mechanical properties is the anisotropic model where the composite contains two phases : the matrix and an aligned, unidirectional reinforcement running the whole length of the matrix. This is also called the Voigt model (Figure 2.4) when the reinforcement is considered running parallel to the force applied, and the Reuss model if the reinforcement is perpendicular to the force. The strain in each phase is considered the same and the composite's stiffness (E_{com}) can be calculated as weighed moduli of the two components, depending on the volume (V_f) fraction of the two components (1 and 2).

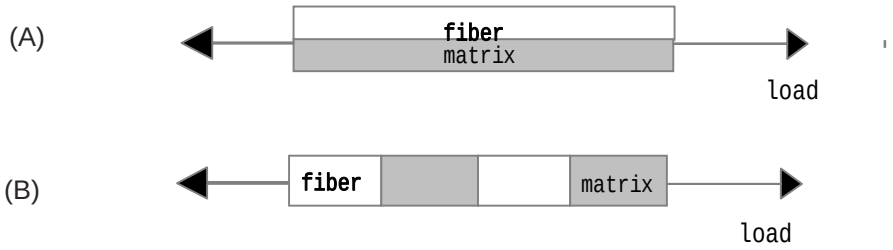

Figure 2.4 – (A) Voigt's model (B) Reuss model of two phases. Adapted from Harris (1999).

Voigt's Equation: $$E_{com} = E_1V_1 + E_2V_2$$

Reuss Equation: $$\frac{1}{E_{com}} = \frac{V_1}{E_1} + \frac{V_2}{E_2}$$

Where E_1 and E_2 refer to Young's modulus of each component and V_1 and V_2 to the volume fraction of components when $V_1 + V_2 = 1$. These values represent the maximal and minimal theoretical values of the modulus for an anisotropic simple composite, which also shows the directional dependence of the modulus of the composites. (Kazt 1996, Harris 1999, Hull and Clyne 2002)

Composite materials often have an isotropic (non-uniform in direction) orientation of reinforcement and even discontinuous reinforcement (short fibers and particles), where the determination of the modulus becomes a more complex process. The discontinuous reinforcement creates peak stress at the edges of the reinforcement - the load transfer from the reinforcement to the matrix and back – thus decreasing the modulus. The modulus for a discontinuous and randomly oriented composite is described by the following equation:

$$E_{com} = E_1V_1 + KE_2V_2$$

where the K represents the fiber efficiency parameter (Krechel's factor) for the reinforcement. The

principle of Krechel's factor is presented in Figure 2.5, where the highest value is for the anisotropic material with fibers running parallel to the direction of the force applied. The lowest value is given to the reinforcement running perpendicularly, as the reinforcement breaks the continuity of the matrix and thus the strength is dependent on the remaining matrix strength and interfacial strength between the matrix and the reinforcement. Randomly oriented (isotropic) reinforcement gives strength in all directions (3D) of force applied. (Harris 1999, Vallittu 2001, Hull and Clyne 2002)

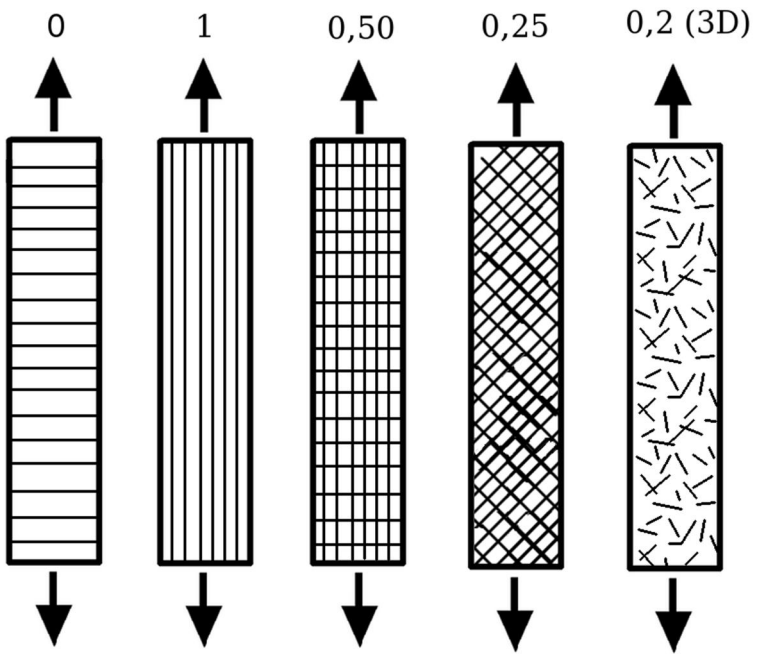

Figure 2.5 – Efficacy of fiber reinforcement according to the orientation (Krechel's factor), when force (F) is applied in the direction of arrows. Adapted from Vallittu (2001)

The strength of bonding between the matrix and the reinforcement also depends on whether the composite is made by the addition of reinforcement to already polymerized material (particles or pellets) and produced, for example, by melt extrusion process – thermo-mechanical method – in which case the attachment is generally mechanical; or if the reinforcement is added to the soluble phase as the matrix is beginning to polymerize – physico-chemical method – there is a stronger chemical-type bond formed between the matrix and the polymer. (Wang 2003) Many factors affect the final strength of the composite, and often there is a gap between theoretical and measured values. This has been explained by inconsistencies in the matrix production (mixing, post curing), flaws in the reinforcement (breaks/cracks), non-uniform reinforcement distribution (matrix rich regions), pores in the matrix (voids), incomplete bonding (between matrix and reinforcement) and internal oxygen inhibition of polymerization of the resin matrix. (Vallittu 1995, Vallitu 1997, Harris 1999, Vallo et al. 2000, Hull and Clyne 2002, Abdulmajeed et al. 2011)

2.3.1. Types of fiber reinforcement

To improve the properties of PMMA-based bone cement, various additive fibers have been incorporated into the polymer. Typically, stainless steel fibers, glass fibers, carbon fibers, polyethylene fibers, aramid (kevlar-related) fibers and titanium fibers have been used. Table 2.1 presents some typical fiber-reinforcement materials and their mechanical properties used in medical implants.

Attempts to enhance the strength of the PMMA-based bone cement with addition of metal wires are reported as early as in the 1970's. With the addition of chopped steel wires, Fishbane and Pond (1977)

reported a 91% increase in fracture toughness. Since then, many reports have shown the addition of steel wires to increase the tensile strength, fracture toughness (up to 2.6 x), and also the enhancement of durability and shrink-resistance when compared to normal PMMA. (Taitsman and Saha 1977, Vallittu et al. 1995, Kotha et al. 2004) The Strength of the composite has been shown to increase by 20%–60% with the addition of titanium fibers, whereas fracture resistance increased by 15-30%. (Kotha et al. 2006, Khaled et al. 2011)

Carbon fibers, graphite and carbon nanotubes are chemically inert, flexible and very resistant to stretching and compression. Carbon nanotubes possess 50-100 times the strength when compared to conventional steel fiber of the same weight (Marrs et al. 2005). According to Saha and Pal (1986), carbon fiber increased the tensile strength and modulus of PMMA cement by 30% and 35.8% respectively, but compression strength and modulus only 10.7%. Marrs et al. (2005) have incorporated carbon nanotubes into PMMA cement and concluded that already a 2 wt % addition enhanced the flexural strength by 12.8% and produced a 13.1% enhancement in yield stress, but above all it increased fatigue resistance by 3.3 times compared to unreinforced cement.

The Addition of ultra high molecular-weight polyethylene (UHMWPE) has been reported to improve the impact strength of the PMMA composite, while the modulus and tensile strength were not markedly enhanced (Vallittu 1996). However, when Ramos et al. (1996) studied surface-conditioned (plasma-treated) polyethylene fibers,they reported almost a 50% increase in strength when compared to conventional PMMA.

The use of E-glass fibers as reinforcement has been studied widely. Stipho (1998) studied the effect of fiber content and found an addition of 1%-wt glass fiber concentration to give the best fracture strength and deformation results, but larger fiber concentrations to cause inconsistencies in the material and weaken it – voids, clumping, incomplete matrix adhesion, etc. This has later been revoked by many authors who have reported an increase in the elastic modulus and the strength of the composite with fiber content up to 40-60%-wt, with precise manufacturing of the composite, including pre-treatment of the fibers (pre-wetting, coating and silane treatment). It is concluded that the best biomechanical properties are gained with unidirectional fiber placement. (Vallittu 1997a, Vallittu 1999, Karasaer et al. 2003, Kim et al. 2004, Narva et al. 2005, Dyer et al. 2005, Tsue et al. 2007) The Silane treatment of fiber glass is used to improve the interfacial bonding between the reinforcing fiber and polymer matrix. The silane agent contains two ends – one of which is capable of forming a bond with the inorganic glass and the other end has organic properties to bond chemically with the PMMA matrix. This is essential for durable, long lasting attachment. (Vallittu 1997b, Wang 2003, Matinlinna et al. 2004, Basant and Reddy 2011)

The porosity of fiber-reinforced implants has been shown to increase bone bonding in an experimental setting piste (Mattila et al. 2006, Mattila et al. 2009, Nganga et al. 2011) A Porosity formation on a solid material can be achieved in many ways by incorporating porogen materials into the matrix as presented in table 2.2. (Chevalier et al., 2008) As an organic material, the PMMA matrix does not permit sintering in high temperatures (evaporation), but allows other methods of porosity formation. Especially the addition of a hydrophilic filler material (polyamines, carboxymethyl cellulose, starch, sugar, etc piste) during polymerization - which dissolves quickly in aqueous surroundings, leaving a porous network – has been studied widely. (Bruens et al. 2003, Puska et al. 2005, Boesel et al. 2006) Another option is to choose a soluble (copolymer or biomaterial) to be dissolved after implantation, but this has been assessed too slow a process to allow adequate cellular ingrowth. (Puska et al. 2005) Dissolving the matrix PMMA partially in a controlled fashion has been presented as a viable option in resent studies. (Aho et al. 2004, Mattila et al. 2004, Hautamäki et al. 2008).

Table 2.1 – Mechanical properties of typical reinforcing fibers - adapted from Harris (1999)

Material	Trade name	Density (10^3kg/m^3)	Fibre diameter (μm)	Young's Modulus (GPa)	Tensile Strength (GPa)
Steel Wire		7.8	250	210	2.8
Glass	E-glass	2.5	10-20	70	1.5-2.0
Aromatic polyamide	Kevlar 49	1.5	12	130	3.6
Polyethylene (UHMW)	Spectra 1000	0.97	38	175	3.0
Carbon	T800	1.8	5.5	295	5.6

Table 2.2 – Methods of creating porosity into a solid material, adapted from Chevalier et al (2008)

Type of process	**Casting**		**Solid (compaction/ extrusion)**
Method	Direct (no sintering)		Indirect (sintering)
Nature of porogen	Gaseous	Liquid	Solid (dispersed powder)
Removal of porogen	Heating Sublimation Evaporation Melting Calsination		Dissolution During process/ In situ

2.3.2. Experimental/preclinical studies

Most studies conducted on non-resorbable composite materials, which are reported as weight-bearing bone defect models, are actually done on non-weight-bearing (cancellous bone or metaphyseal wedge defects) or partial cortical defect models. (Dean et al. 1999, Wheeler et al. 2000, Ignatius et al. 2001, Abu Bakar et al. 2003)

Experimental studies on a critical-size bone segment repair with polymer composites in weight-bearing surroundings are limited in number. Critical-size bone defect models in weight-bearing surroundings are difficult to construct, as the size of the defect required varies from species to species, which makes the studies often lacking in quality (Reichert et al. 2009). Fiber-reinforced composites (FRC) have been used in critical-size bone defect models, where they have been proven to be durable and well incorporated into the host bone. Tuusa (2007 and 2008) reported an FRC with a bioactive glass coating to work well in a rabbit calvarial bone defect model, with no adverse inflammatory reactions and good new bone formation. Mattila (2009) reported an FRC implant with a porous surface - used in a metaphyseal defect model – to have increased the bone bonding capabilities when compared to a conventional PMMA or Ti-alloy implant. Aho (2004) and Hautamäki (2008) have reported the use of an FRC implant with a porous surface in a critical-size defect model - in weight-bearing surroundings - on a rabbit's tibia. The

results of short- and long-term follow-up have shown no adverse inflammatory reactions and good bone incorporation, and the implant has withstood well the strain induced to it, as no implant breakages have occurred.

2.3.3. Clinical studies

Clinical studies on critical-size bone defects using polymers or polymer composites are scarce, and often limited to case reports or series of patients. Eppley et al. (2002) have reconstructed the cranial defects of 14 patients with a computer-modeled pre-prepared PMMA-based scaffold with good results in even a 7-year follow-up . A 20-year follow-up was reported by Bruens et al. (2003) where they used in situ a polymerized porous PMMA composite. 24 patients were primarily treated for cranial defects with a direct application of the cement – bony lesions and complete lesions to the dura - with no adverse reactions after the operations. Saringer et al. (2002) and also Wurm et al. (2004) have reported the use of custom-made carbon fiber-reinforced polymer scaffolds used on patients with cranial defects. With up to a 7-year follow-up, only a few failures have been experienced, and most of them were infectious.

A custom-made PMMA implant with a bioglass surface to replace large cranial defects in four patients has been reported by Peltola et al. (2012). The PMMA core was prepared according to a 3D –CT image, perforated and coated with bioactive glass to enhance bone incorporation. During the preliminary 2-year follow-up, no failures have been experienced.

3. AIMS OF THE PRESENT STUDY

The aim of this study was to develop a fiber-reinforced composite (FRC) implant for segment defect repair in weight-bearing surroundings. The implant's biomechanical properties were adjusted to minimize stress shielding between bone and implant. The surface properties were optimized to allow bone growth onto the material with a newly developed solvent treatment method. The New implant was tested for safety and biocompatibility, and the properties for attachment to bone were evaluated. The general working hypothesis was that the FRC implant could provide biocompatibility and biomechanics, which can be utilized in the repair of long bone defects.

The Specific aims of the studies were:

I To develop an FRC implant with a porous surface structure, test its biomechanical properties compared to bone, and evaluate the behavior of the implant in a bone segment defect repair model in a short follow-up .

II To evaluate the FRC implant's behavior in a long-term setting (8 and 20 weeks) in comparison to a plain PMMA implant, and assess the histological reactions and bone bonding with the new bone contact index (BCI) method.

III To evaluate the biocompatibility of the developed FRC implant in a cell culture model with soluble markers and cellular function, cell division and formation of calcium precipitates with SEM analysis

IV To evaluate the effects of the orientation of the fiber reinforcement on the solubility of the FRC, and assess how the solvent treatment affects the bone bonding capabilities of the FRC.

4. MATERIALS AND METHODS

4.1. Materials

Materials used for the manufacturing of the test specimens are listed in Table 4.1 and the types of specimens manufactured are specified in Table 4.2

Table 4.1 – materials used in the studies

Brand	Type	Manufacturer	Study
Palapress®	PMMA powder[a]	Heraeus Kulzer GmbH and Co KG, Hanau, Germany	I,II, III, IV
Methyl methacrylate (MMA)	Monomer	Sigma-Aldrich Chemie GmbH, Steinheim, Germany	I,II, III, IV
DMPT (N,N-dimethyl-p-toluidine 99%)	Activator	Sigma-Aldrich Chemie GmbH, Steinheim, Germany	I,II, III, IV
Stick®	Pre-impregnated E-glass fibres[b]	Stick Tech Ltd, Turku, Finland	I,II, IV
BG granules	Bioactive glass (S53P4)[c] granules, size 315-500 µm	Vivoxid Ltd, Turku, Finland	I, II, III
Tetrahydrofuran (THF)	Solvent	JT Baker, Deventer, Netherlands and Sigma-Aldrich Laboratoriochemicalen GmbH, Seelez, Germany	I, II, IV

[a] Poly(methyl metacrylate -co-methacrylate)copolymer with average molecular weight M_w 220.000. The product contains benzoyl peroxide radical as initiator

[b] E-glass fibers (electrical glass) with composition SiO_2 54w%, Al_2O_3 14w%, B_2O_3 6w%, with small amounts (<1,0w%) of MgO, Na_2O, K_2O (stated by the manufacturer). Fibers had on average, a 16µm diameter and were silanated and polymethyl methacrylate preimpregnated.

[c] Bioactive glass (S53P4) composition: SiO_2 53w%, Na_2O 23w%, CaO 20w% and P_2O_3 4 w%.

Table 4.2 - Types of specimens manufactured for the study

Study	Type of specimen	Group Codes	Method of testing	Dimensions	Number of specimens
I	Prepolymerized PMMA[a] rods (with and without E-glass[b] fiber reinforcement)		Three point bending (flexural strength and modulus of elasticity)	2 x 2 x 25mm^3	n=6 / group
I , II	Prepolymerized tubular implants - Plain PMMA[a] - Fiber[b]-reinforced PMMA[a] with a porous surface and bioactive glass[c] granules	 - PMMA - SP-FRC	Experimental segment defect repair with the implant (an animal model with a follow-up of 4, 8 and 20 weeks)	Tubular implants 6-7mm width, 10mm height and a 3 mm hole running in the center longitudinally	Plain PMMA n=4 / time-point SP-FRC (n=5 at 4 weeks, n=5 at 8 weeks, n=10 at 20 weeks)
III	Prepolymerized specimen disks - Smooth surface PMMA[a] - Rough surface PMMA[a] - Rough surface PMMA[a] with bioactive glass[c] granules	 - S-PMMA - R-PMMA - BAG-PMMA	Cell cultures with rat osteoblasts (follow-up times 1, 7, 14, 21 days)	3 x 12mm (height x diameter)	n=4/ group, for each of the time-points
IV	Prepolymerized PMMA[a] sheets (with and without E-glass[a] fiber reinforcement) - vertically oriented fibers - horizontally oriented fibers - randomly oriented fibers - no fibers	 - Group V - Group H - Group R - Control	-Dissolution by THF (surface porosity creation) -Pullout strength (experimental bone bonding)	15 x12.3 x 0.45mm (length x width x thickness)	n= 6/group /time-point

[a] Poly(methyl metacrylate -co-methacrylate)copolymer with average molecular weight M_w 220.000. The product contains benzoyl peroxide radical as initiator

[b] E-glass fibers (electrical glass) with composition SiO_2 54w%, Al_2O_3 14w%, B_2O_3 6w%, with small amounts (<1.0w%) of MgO, Na_2O, K_2O (stated by the manufacturer). Fibers were had, on average, a 16µm diameter and were silanated and polymethyl methacrylate preimpregnated .

[c] Bioactive glass (S53P4) composition: SiO_2 53w%, Na_2O 23w%, CaO 20w% and P_2O_3 4 w% .

4.2. Methods

4.2.1. Fabrication of FRC with a porous surface (studies I, II and IV)

A method of manufacturing a polymethyl metacrylate (PMMA)-based implant with fiber reinforcement and a porous surface structure for long bone defect repair in an animal model (studies I and II) was developed. A supplementation of bioactive glass (BG) (S53P4) was added to the material during the process to enhance bone growth onto the implant. The implant was made to a shape which simulated a section long bone with a tubular form (medullary canal) and a triangular cross-sectional shape to match the tibia of a rabbit.

The core of the implant was made of autopolymerizing polymethyl methacrylate (PMMA) (Palapress® Heraeus Kulzer, Wehrheim, Germany) resin (PMMA powder/ MMA monomer liquid; powder-to-liquid ratio 1:1). The polymer resin was placed in a polyvinyl siloxane mold with continuous unidirectional E-glass (21w%, Stick®, Stick Tech Ltd, Turku, Finland) running longitudinally in the implant, and a small plastic tube in the middle simulating a medullary canal. The mixture was polymerized in a pressure curing device at 200kPa (15 minutes in 55±3°C) (Ivomat, Typ IP 2, Ivoclar AG, Schaan; Lichtenstein). After curing, the bulk core was immersed in a mixture of

tetrahydrofuran (THF) solvent (Sigma-Aldrich Laboratoriochemicalen GmbH, Seelez, Germany) 10ml and PMMA powder (0,69g) (Palapress®) for 5 seconds, after which water was added to create emulsion-like foam around the core. During this foam-formation process, the BG granules (S53P4, size 315-500 µm) (Vivoxid Ltd, Turku, Finland) were adhered to the surface. The porous surface was created in a combination of dissolving of the surface of the PMMA core and adhesion of the PMMA powder foam under the influence of the THF solvent and water. The implant was left to dry in order to let the THF and the water to evaporate. After drying, the implant was formed by manual grinding to reach its final shape and dimensions (diameter 7-9 mm and length 10mm). Control implants were made of pure PMMA without any reinforcing fibers or BG, and the surface was only ground with a metal file. All the implants were water stored for at least 24 hours before use to remove any monomers and activators remaining from the polymerization. Figure 4.1 illustrates the implant's structure and appearance.

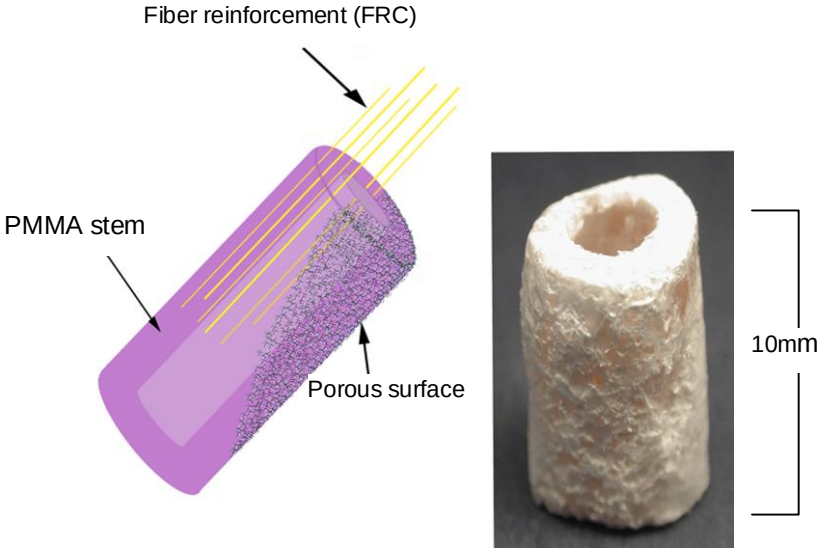

Figure 4.1 – Schematic drawing of the FRC implant and a macroscopic appearance of the finished implant

In study IV, an improvement to the method of creating surface porosity through surface dissolution process, with the effect of differently oriented fiber reinforcement, was explored. For this study, four types of specimens were manufactured (four specimens per group), with an average size of 15 x12.3 x 0.45mm^3 (length x width x thickness). The first group of specimens had unidirectional and continuous fibers running vertically (Group V) along the long axis of the specimen, whereas the second group of specimens had the fibers crossing perpendicularly (Group H) to the long axis of the specimen and the third group had randomly oriented short (approximately 2mm of length) fibers (Group R) in the specimen. The test specimens of the fourth group were made solely of PMMA and served as controls (Group C). The test specimens were made in a mold using components described in Table 4.1. For the groups V and H, the E-glass fibers (Stick®) were cut to the length/width of the mold (weighing 0.180g for each mold). The fibers were separated and laid into the mold, and a mixture of 5g of PMMA powder containing initiators and 3.5 ml of liquid (MMA) monomer containing 2 wt% of DMPT (N,N - dimethyl-p–toluidine) as activator was poured over them. The fibers for the group C were cut to the length of 2mm (chop) and blended together with the PMMA – MMA-DMPT mixture before being poured into the mold. A glass sheet was placed on top of the mold before the final polymerization in a pressure curing device (Ivomat, Typ IP 2, Ivoclar AG, Schaan, Liechtenstein) (15 minutes, 200kPa, +55 °C). The rough specimens were cut into the final shape with a laboratory band saw and smoothed with circular rotating grinder (LabPol-21, Stuers A/S, Rodøvre, Denmark) with 1200 grit silicon carbide abrasive paper (Stuers A/S; Rodøvre, Denmark). The dimensions (length x width x thickness) of each specimen were recorded by a digital caliber to an accuracy of 0.01 mm and the specimen was marked for later identification.

After manufacturing, the test specimens were placed between two microscope/thin glass sheets longitudinally with one end extending 9mm beyond the edge of the glass sheets. The formed specimens were suspended in a container (3 specimens / container) and 5 ml of THF was applied to the bottom. The specimens were placed in a manner that allowed the ends to be in contact with the solvent, without immersing the entire

specimens. The container was sealed for the duration of 5, 15 or 30 minutes, according to the protocol. The specimens were removed from the container and left to dry/so that the THF evaporated from the specimens. The propagation of the dissolution was measured by determining the remaining – not dissolved – final longitudinal length of the specimen. The change in width and thickness was also observed. Figure 4.2- illustrates the dissolution test setup, and 4.3 the specimens and Figure 4.4 the measurement of the specimens.

4.2.1.1 – Staining test for capillary formation

The dissolving of the matrix was suspected to create capillary channels along the fiber reinforcement into the specimens, before it changed the actual height of the specimens. This phenomenon was verified by a staining test, and as the PMMA is hydrophobic, the staining liquid consisted of Patent Blue (E131) and ethanol (EtOH, 40- w%). The 15-minute dissolution specimens were immersed into the staining agent for 15 minutes, after which their surface was gently wiped and they were left to dry.

4.2.1.2 – SEM imaging

A scanning electron microscope (SEM) (JSM-5500 JEOL, Tokyo, Japan) was used to evaluate the surface structure of the test specimens. The implants for the segment defect repair (studies I and II) were either split longitudinally or cross-sectioned with a circulating band saw and polished with a rotating grinder (LabPol-21, Stuers A/S, Rodøvre, Denmark). The surface dissolution test (study IV) specimens were used as they were. The specimens were sputter coated (BAL-TEC SCD 050 Sputter Coater, Balzers, Liechtenstein) either with a layer of gold or carbon.

4.2.2. Biomechanical testing

4.2.2.1. – Properties of the FRC (study I)

The specimens were prepared in two groups: the first group with a longitudinal unidirectional E–glass fiber (45w%) (Stick®) reinforcement and the second without the fibers. Six specimens were prepared for each group. PMMA /MMA resin (Palapress®) - with liquid-to-powder ratio 1:1 - was inserted to a stainless steel split mold (with or without the fibers) and polymerized in a pressure curing device (Ivomat, Typ IP 2, Ivoclar AG, Schaan, Liechtenstein) for 15 minutes (200kPa, +55 °C). The specimens were wet-ground to the dimensions of 2x2x25 mm^3 (±0.1mm) with 1200 grit silicon carbide grinding paper, using a grinding machine (LabPol-21). After being stored in dry for at least 24 hours, the flexural properties of the specimens were tested with a three point bending test (according to the ISO 10477 standard). The span between the supports was 20.0mm, and a load was applied to the middle of the specimen by an universal testing machine (Lloyd LRX Lloyd Instruments Ltd, Fareham, England) with a 1mm/s crosshead speed.
The load and deflection of the specimen were recorded using the Lloyd Nexgen (Lloyd Instruments Ltd, Fareham, England) program, and the fracture load was measured and used to calculate the flexural strength (*S*), toughness and flexural modulus (*E*) of the specimens according to the following formulas.

$$S = \frac{3FL}{2bd^2}$$

where S= strenght (MPa), F = load at break/yield (N), L = span of the specimen between supports (mm), b= width (mm), d = thickness (mm)

$$E = \frac{F_1 L^3}{4bd^3 D_1}$$

E = modulus (GPa), F = force at point D_1 (N), L = span of the specimen between supports (mm), b = width (mm), d = thickness (mm), D_1 = deflection at linear region of the load-deflection curve (mm)

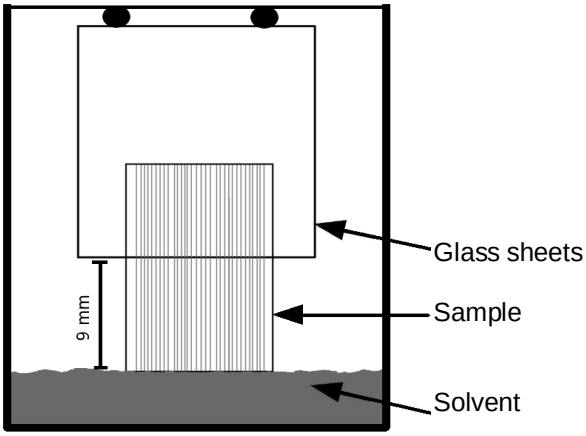

4.2 – Dissolution test setup

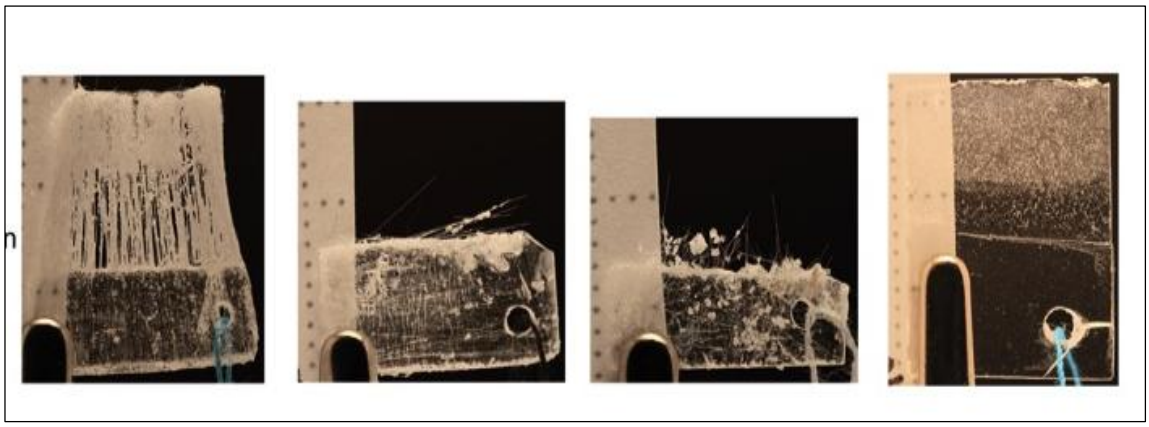

Figure 4.3 – Test specimens displaying the effect of 30 minutes of solvent treatment (from left to right: vertical, horizontal, random, control)

Figure 4.4– Photograph displaying the measurement of the specimens after the solvent treatment

4.2.2.2. – Experimental bone-bonding strength (study IV)

Specimens from the dissolution test (study IV) were used to experimentally evaluate the bonding strength of a porous-surface FRC material in comparison to plain PMMA, when they were partially embedded in plaster of Paris (Mattila et al. 2006, Nganga et al. 2011). The specimens (6 / time-point /Group) with exposed glass fibers were embedded in dental stone (GC Fujirock ® EP, GC Europe, Leuven, Belgium) held in molds. The dental stone was prepared as follows: a powder-to-liquid ratio of 100g powder to 20 ml distilled water was used, as recommended by the manufacturer. The powder and water were mixed for 45 seconds and the mixture was poured into cylindrical nylon molds (height 20mm, diameter 25 mm). The specimens were embedded in the plaster to the depth of three millimeters (Figure 4.4), ensuring that all of the spaces between the exposed fibers were filled with the plaster of Paris. After an initial setting time of 15 minutes, the plaster of Paris was left to age for 3 days (NTP) before the pullout testing.

For the pullout testing, the mold with the specimen was fixed to a universal laboratory testing machine (Lloyd, model LRX, Lloyd Instruments, Fareham, England) and the top half was clamped tightly and attached to the device. (Figure 4.5) The test was made in air with a loading speed of 1mm/s, until breaking of the bond between the specimen and dental stone, or the breaking of the specimen itself. The maximum force was registered in newtons (N), and a bonding/tensile strength was calculated with the machine's software.

a)  b) 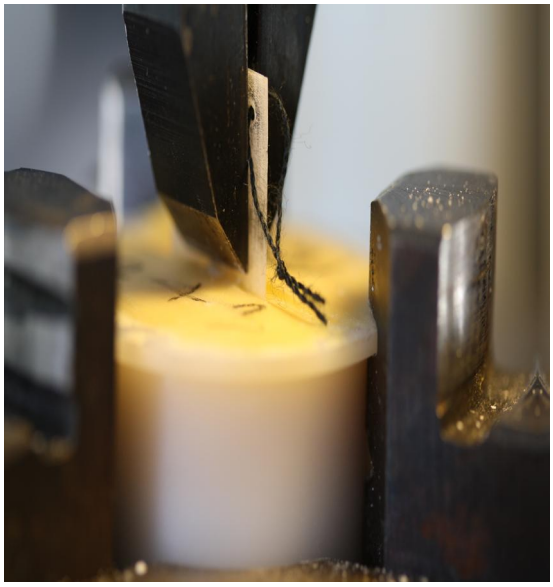

Figure 4.5 – a) The holding device for curing the specimens and b) the set up for pullout testing, where the pulling clamp is holding the specimen and the mold is attached to the vise on the machine.

4.2.3. Biocompatibility testing – In vitro (study III)

4.2.3.1. Preparation of cell culture specimens

Plain PMMA specimens and composites with bioactive glass granules were prepared as follows. PMMA powder, containing benzoyl peroxide initiators and MMA monomer containing 2 w% DMPT as activator, were mixed (liquid-to-powder ratio 1:1). For bioactive glass containing specimens (BG-PMMA), a 30 w% of granules (S53P4, size: 315-500 µm) was added to the mixture. The mixture was poured into a mold of a cylindrical shape, and it was polymerized in a pressure curing device (Ivomat, Typ IP 2, Ivoclar AG, Schaan, Liechtenstein) for 20 minutes (400 kPa, 90 ± 3□C). The polymerized solid cylinder (diameter: 12 mm) was sawed into disks (height: 3 mm). All BG-PMMA composite disks were roughened with a 180 grit silicon carbide grinding paper. Half of the plain PMMA disks were roughened (R-PMMA) with 180 grit silicon carbide grinding paper, and the other half (S-PMMA) were polished with 2400 grit, using a grinding machine. All the specimens were ultrasonically cleaned with 70% ethanol for 5 minutes and washed with distilled water before being sterilized in an autoclave at 120°C for 20 min. Conventional tissue culture polystyrene (TCPS; Costar, Corning Inc, NY) wells were used as controls.

4.2.3.2. Osteocyte cultures

The stromal cells of a rat's bone marrow were harvested and cultured according to Maniatopoulos et al. (1988). In short, the femurs of three young adult male Sprague-Dawley rats were isolated. The bones were wiped with 70% alcohol and immersed twice in an α-MEM (Sigma Chemical Co., USA) culture medium containing 100 units/ml of penicillin/streptomycin (Gibco BRL, Life Technologies BV, The Netherlands). The condyles were cut off and the bone marrow was flushed out using complete cell culture medium (α-MEM and antibiotics supplemented with 15% fetal bovine serum (Gibco BRL), 50 µg/ml ascorbic acid (Sigma Chemical), 5 mM Na-β-glycerophosphate (Merck, Germany), and 10 nM dexamethasone (Sigma Chemical). The resulting suspension was passed through a 22 gauge needle, and plated cells were cultured in a humidified 5% CO2 atmosphere at 37°C.
After seven days of primary culture, the adherent cell population was trypsinized and resuspended in a complete culture medium. The polymer and composite substrates were washed once with phosphate buffered saline (PBS) and once with a culture medium at 37°C, for one hour each. Cell suspension was subsequently added on the test substrates at a density of 25 000 cells/cm^2, and cells were allowed to adhere over night. After seeding, the osteoblast culture was continued for three weeks in 24-well plates with a medium replacement every 2 to 3 days. The culturing of cells in each specimen group was terminated (on day 1, 4, 7 and 14) and the specimens were placed in a desiccator to dry them. The dried specimen discs were sputter coated (Bal-Tech) with carbon and inspected with a scanning electron microscope (JSM 5500). The proliferation and differentiation of the osteoblasts was evaluated, as well as the production of extracellular matrix/calcifications.

4.2.3.3. Cellular activity

The proliferation of cultured cells was determined using the AlamarBlueTM assay (BioSource International, Camarillo, USA) in a colorimetric format. The specimens (n=4) were withdrawn from the culture at predetermined time-points, washed in PBS, and placed in clean 24-wells. A fresh culture medium with 10% assay reagent was added to the wells, and after three hours of incubation, the absorbance values of the medium were read at 560 nm and 595 nm using an ELISA plate reader (Multiskan MS, Labsystems, Helsinki, Finland). The measured absorbances were used to calculate the reduction of the assay reagent, and the cell activities were normalized in respect to those on TCPS at the first time-point – day 1 represents 100% activity.

The Calcium concentration changes in the culture medium were determined using a orthocresolphthalein complexone (OCPC) method (Lorentz, 1982), where low calcium concentrations in the medium indicated high osteoblast mineralization. The assay reagent consisted of OCPC with 8-hydroxyquinol in an ethanolamine/boric acid buffer. Absorbances were taken at 560 nm using the ELISA plate reader and calcium concentrations were obtained from a $CaCl_2$ standard curve.

At predetermined time-points, total cellular RNA from TCPS control wells and polyA mRNA from the experimental culture substrates were isolated using Trizol® reagent (Gibco) and QuickPickTM mRNA magnetic beads (Bio-Nobile Oy, Parainen, Finland), respectively. Three replicate RNA pools from each substrate type were reverse transcribed (RT) with random hexamer primers using a GeneAmp Gold RNA PCR Reagent Kit (Applied Biosystems, Carlsbad, USA). The resultant first-strand cDNA was analyzed in duplicate PCR reactions using an iQ Supermix kit (Bio-Rad Laboratories) and FAMlabeled TaqMan® Gene Expression Assays (Applied Biosystems) for bone sialoprotein (BSP), osteocalcin (OC) and glyceraldehyde-3-phosphate dehydrogenase (GAPDH) as control. The PCRs were carried out using an iCycler iQ real-time PCR detection system with software version 3.1 (Bio-Rad Laboratories, Helsinki, Finland). The threshold cycles (CT) were automatically calculated using “the maximum curvature approach”, and the gene expression levels of BSP and OC were normalized to a GAPDH expression in each RNA pool (ΔCT = CT, target – CT, GAPDH). A difference of one unit in ΔCT values corresponds to a two-fold difference in gene expression level.

4.2.4. Animal experiments (study I-II)

Animal experiments were carried out to evaluate the FRC implants' behavior in an in vivo setting. A model with a critical-size bone segment defect simulating a true clinical case, where a bone tumor has been resected with large margins from a weight-bearing bone, was chosen. This kind of defect does not heal by itself, and has ordinarily been replaced with a tumor prosthesis made of metal. A larger animal should be chosen for this experiment – a lamb, pig, dog or a rabbit - as the size-to-weight ratio and the axial loading pattern of the limbs resemble those of a human. The bone size and quality has to be taken into account, as bones too small and fragile do not allow adequate fixation methods. In addition, a larger animal has a longer life span and a similar slow turnover rate and healing capabilities in bones as humans. Using a rabbit as a test animal for a load-bearing model has limitations. The forearm of a rabbit is thin/narrow and the loading on the forearms is also limited, as the animal’s weight is supported mainly by its hind limbs while moving and especially when standing. The axis of a rabbit's femur is constantly horizontally oriented and no true axial loading is achieved. The tibia of a rabbit is of good size and has a large medullary cavity to house the intramedullary fixation. Moreover, the cortex of the tibia is strong, although thin, and enables cutting, drilling and fixation by screws. Rabbits may not be the optimal choice to be used in a simulating repair of human bone, but our laboratory has previous good experience working with rabbits, as they mature quickly, are easily maintained, and they are also an economically viable option.

The experimental segment defect repair on rabbits was conducted by permission from the Lab-Animal Care & Use Committee, the Central Animal Laboratory, the University of Turku and the Regional State Administrative Agencies of Southwest Finland (no. 51124/7624). The animal experiments were performed according to the Good Laboratory Practise (GLP) quality principles as well as following all the national and European instructions, regulations, applicable guidelines and legislation.
Altogether 32 mature (3,4 – 4kg of weight) New Zealand White female rabbits underwent surgery. The animals were single housed at the Central Animal Laboratory, the University of Turku, 14 days prior to the surgery - to accommodate them to the surroundings - and after the operations for the duration of the study (4, 8 and 20 weeks). The animals were allowed free movement outside the housing for one hour a day in small groups, as they were observed by the animal caretakers for any abnormal behavior.

4.2.4.1. Operative procedure

The surgery was performed in operating room conditions with surgical sterility protocols at the Central Animal Laboratory. General anesthesia was induced by intramuscular injections combining 5 mg midazolam hydrochloride (Dormicum®, Roche Oy, Espoo, Finland), 0.8 mg medetomidine hydrochloride (Domitor®, Orion –Yhtymä Oyj, Espoo, Finland) and 50 mg ketamine hydrochloride (Ketalar®, Pfizer Oy, Espoo, Finland). The fur was trimmed off

the operative area (left tibia) and the area was wiped clean with ethanol-scrub (70 vol%) (Primalco, Helsinki, Finland), and draped sterile. The skin was incised at the medial margin of the tibia, beginning at the tuberosity and continuing 3 cm downwards. Periosteum was split at the tibial ridge and muscles were lifted up with the periosteum. A segment of tibia (10mm legth) was removed below the tibial tuberosity with a water-cooled circular saw. The defect was replaced by the test implant which was fixed to the bone either with intramedullary Kirchner wires or a LC-DCP-plate (Stratec Medical Oy, Helsinki, Finland), after which the wound was closed in layers. Postoperatively, the animals were allowed immediate weight bearing and free movement, and pain was treated with subcutaneous injections of buprenorphine hydrochloride (Temgesic®, Schering-Plough Europe, Brussels, Belgium) of approximately 0.015 mg/day for 3 days.
The animals were euthanized by an overdose of pentobarbital (Nembutal®, Orion Oyj, Espoo, Finland) at predetermined time-points, and the tibias were excised as a whole, the soft tissues were removed and the specimen fixated in ethanol (70 vol%) (Primalco) for further studies. Figure 4.6 displays a schematic drawing of the segment replacement and a photograph of the operated limb.

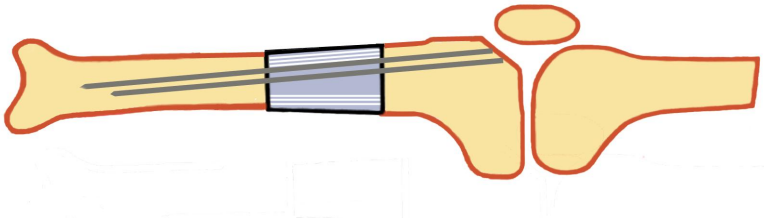

Figurere 4.6 – A schematic drawing of the operated limb, with a segment replaced by the implant and fixed with K –wires.

4.2.4.2. Histological and histometrical analysis

A section of each tibia (~2 cm) containing the implanted area was prepared as a non-decalcified sample. They were first defatted in rising alcohol series (70vol%, 80vol%, 98 vol% - 2 days in each), and then embedded in acrylic resin (Technovit, Kulzer GmbH, Wehrheim, Germany). Acrylic embedded sections of the tibia were then halved longitudinally (anterior-to-posterior plane) and one half was prepared by a cutting –grinding method to a specimen with a 20-µm thickness. The finished specimens were treated by the van Gieson staining method (Donath and Breuner 1982) for a light microscopic analysis.
In the histological specimens, the presence of inflammatory reactions or resorption of host bone was evaluated, and the formation of new bone/mature bone and bone incorporation around the implant was observed.
A histometrical analysis was conducted using a computer-assisted analysis system (Microscale TC; Digithurst Ltd., Royston, UK) to determine the bone growth at different anatomical areas: both longitudinal surfaces, the junctions (interface) between the implant and the cortical host bone, and the marrow canal. A bone contact index (BCI), which is the percentage from the sum of contact lines between bone and implant – at cortical junctions, posterior and anterior surface – of the corresponding total length of the implant, was determined. (Figure 4.7) Total appositional bone growth (ABG) over the posterior surface of the implant is the area percentage of bone measured from the whole area over the posterior cortex of the implant covered by tissue. The porous surface bone growth (PSG) is the area percentage of bone growth into the porous surface, determined from the area rising over the stem on the posterior cortex by 0.4mm, which is the average thickness of the porous surface evaluated from the SEM images. The intramedullary growth of bone (IMG) is the percentage of bone from the total canal area within the implant.

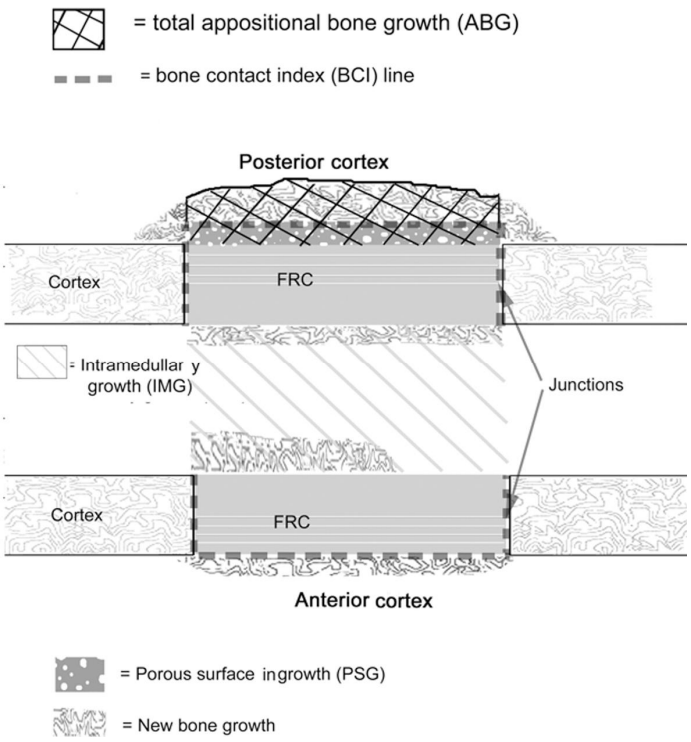

Figure 4.7 - The principles of measuring Bone Contact Index, intramedullary growth, porous surface growth and appositional bone growth.

4.2.4.3. X-ray imaging –observations

Before preparing the FRC specimens for histology, plain non-screen contact radiographs (35 kV and 175 mA) of the whole tibias in anteroposterior and lateromedial views were taken at the Department of Radiology, Turku University Central Hospital. Radiological incorporation, possible resorption of host bone and new bone growth were evaluated around the implant and at the bone-implant junctions.

4.2.5. Statistical analysis (study studies I-IV)

Statistical analysis for the numerical data gathered in the studies was done using the latest available version of the SPSS program (Statistical Package for Social Studies, SPSS Inc., Chicago, IL, USA). In studies I and II , a one-way analysis of variance (ANOVA), a Mann-Whitney U-test and Students-T-test were used, respectively. For the studies III and IV, the data was analyzed with a one-way ANOVA followed by Tukey's post-hoc test. For all of the tests, a P value lower than 0.05 was considered significant (with a 95% confidence interval) after the Bonferoni correction for multiple comparisons.

5. RESULTS

5.1. FRC specimen fabrication (studies I and IV)

5.1.1. Porous surface formation

The creation of porous surface on the implant material was reported in study (I). The newly developed solvent foaming method was successful in creating a porous surface around and inside the canal of the fiber-reinforced core. Macroscopic porosity could be detected in visual inspection, and SEM images of the split and cut surfaces revealed complex porosity, with pore size ranging from 10- 500 µm. The pores were interconnected due to the foaming process and evaporation of H_20 and THF from the material leaving openings into the pores, which was confirmed by SEM images. This was also confirmed in a histological examination, where growth or bone into the surface porosity could be seen (Figure 5.1). The transition layer - from the porous surface to the core of the implant - was very sharp, suggesting that the penetration depth of the solvent foaming treatment did not have an effect deeper in the core (as shown in study IV), and thus the mechanical properties of the core were assumed practically unchanged. The surface of the control implants was only slightly roughened due to the grinding process. Figures 5.2 and 5.3 illustrate the macroscopic and SEM findings.

During the implant preparation and at surgery, an inconsistency and instability of the surface porosity were noticed. Some specimens showed small bald spots or flaking of the porosity on the surface (i.e. the core material was clearly visible), and thinning of the porous surface structure, especially at the ends, as presented in Figure 5.3. These specimens were discarded from animal testing, but were kept for further analysis. These findings led to further development of the porous surface, as seen in study (IV).

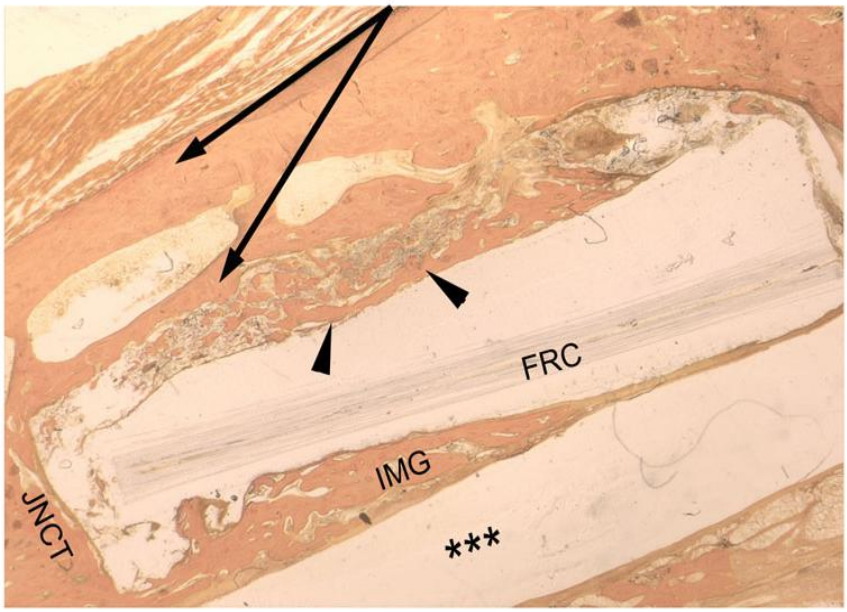

Figure 5.1 – A histological figure of bone growing into the porous surface (arrowheads). Arrows point at new cortical bone growing along the implant. Junction (JNCT) and intramedullary (IMG) growth can be evaluated. (***) is the intramedullary canal showing the empty space left by K-wires.

Figure 5.2- Surface and longitudinally split implant specimen

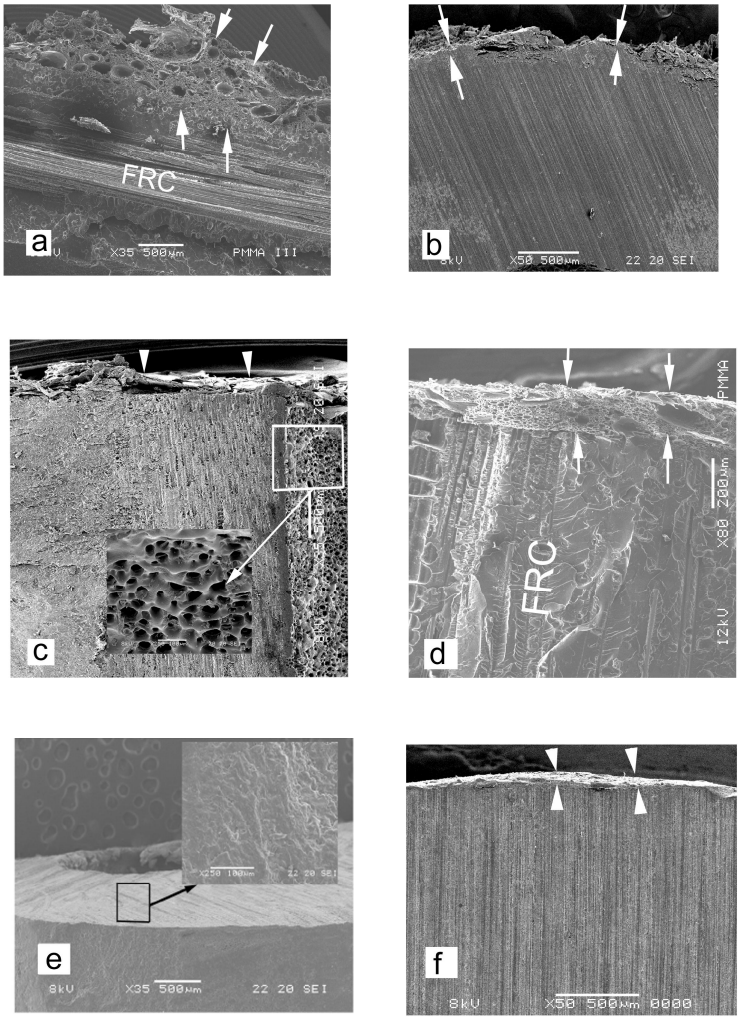

Figure 5.3 – SEM images of the FRC implants and PMMA controls

a) Ideal surface porosity (between arrows) on FRC implant with unidirectional fiber reinforcement (FRC) showing in the core
b) Variable quality of surface porosity (arrows) on the FRC implant
c) Porosity in the intramedullary canal of the FRC implant , with higher magnification (x250) detail
d) The filed end and a higher magnification detail of the control (PMMA) implant
e) The side of the control implant with only a slightly uneven surface (arrowheads)

The surface dissolution testing (study IV) revealed how the fiber reinforcement and the orientation of the fibers in the specimens affected the solution of the matrix. None of the specimens showed noteworthy deterioration of the polymer matrix after 5 minutes of solvent treatment, and only minor changes in the surface could be seen as the material became less transparent and some specimens showed minor cracking of the matrix. After 15 minutes, the Group V showed significantly more dissolving than the other groups ($p<0.001$). The THF solvent had apparently penetrated more rapidly along the longitudinal continuous fibers creating (capillary) canals inside the material, which was confirmed by the additional staining test. The test showed that the staining agent penetrated the matrix by capillary forces in the Group V, as the specimens of other groups did not show corresponding penetration of the staining liquid to the dissolved layer of the specimen. (Figure 5.4) The penetration depth of the solvent THF was increased when the contact time with the solvent was prolonged, but not linearly. (Figure 5.5) After 30 minutes of the solvent treatment, all of the fiber-reinforced specimens´ groups (V, H and R) showed a significantly higher depth of solvent penetration than the specimens of the control group ($p<0.001$). The specimens without glass fibers showed only minor deterioration on the surface - crazing and cracking - after 30 minutes of treatment. (Figure 5.6 and 5.7)

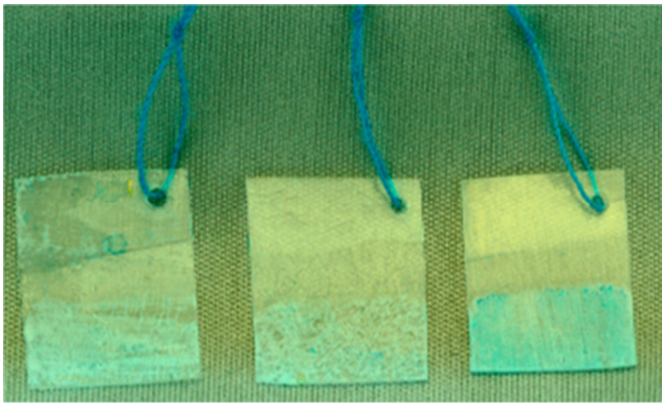

Figure 5.4 – Staining test samples (from left to right: Group H, Group R and Group V) after 15 minutes of dissolution, clearly showing the advancement of the staining agent - Patent Blue (EtOH 40%-vol) - higher in Group V than in the others.

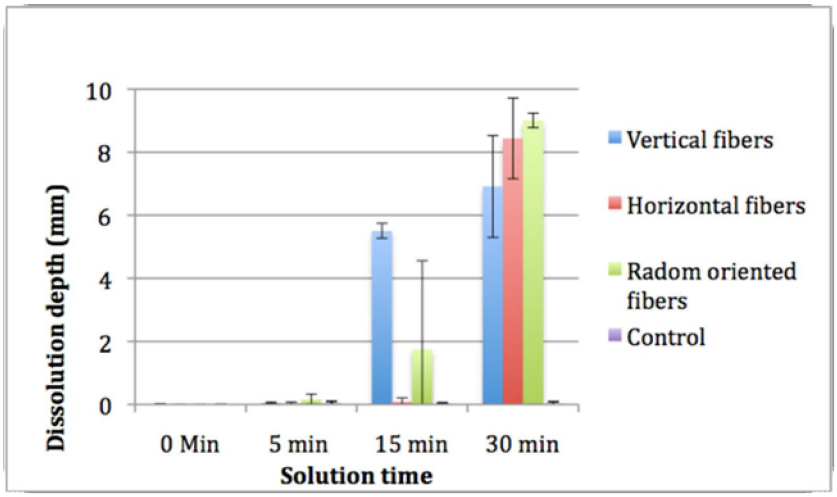

Figure 5.5 – Diagram showing the advancement of dissolution in the samples as function of time. Whiskers represent ±1 SD.

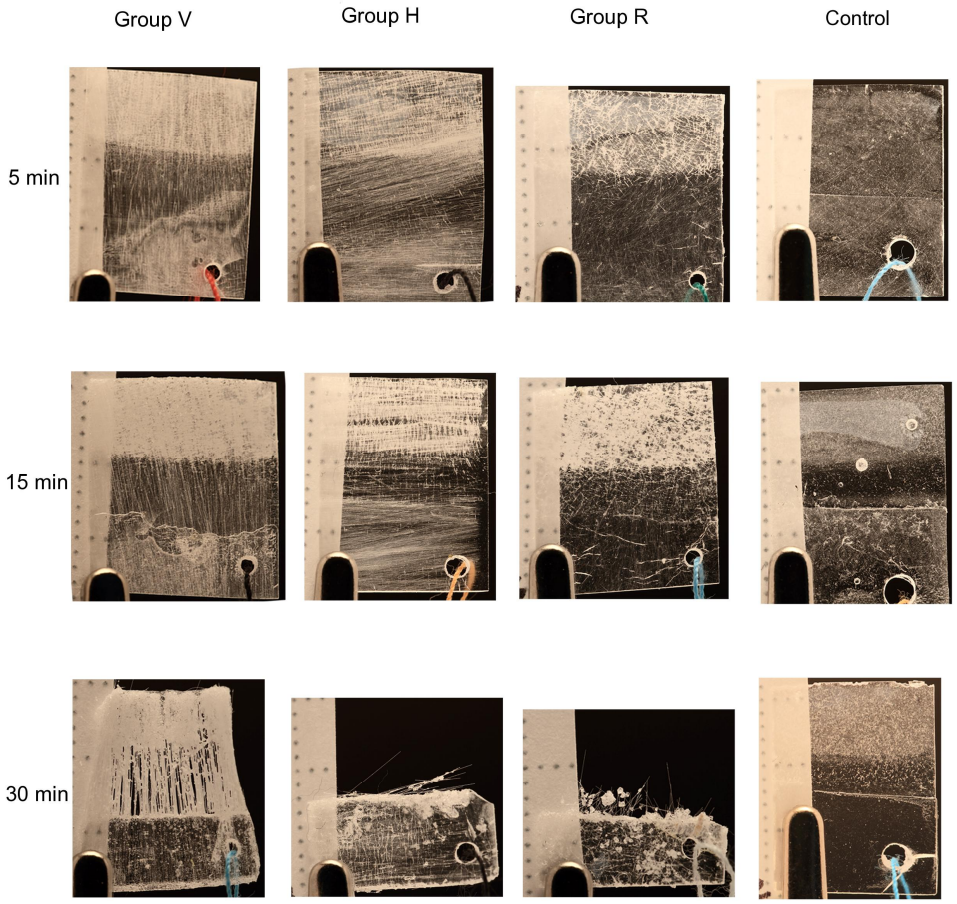

Figure 5.6 – The dissolution test specimens at different time points. Macroscopic images.

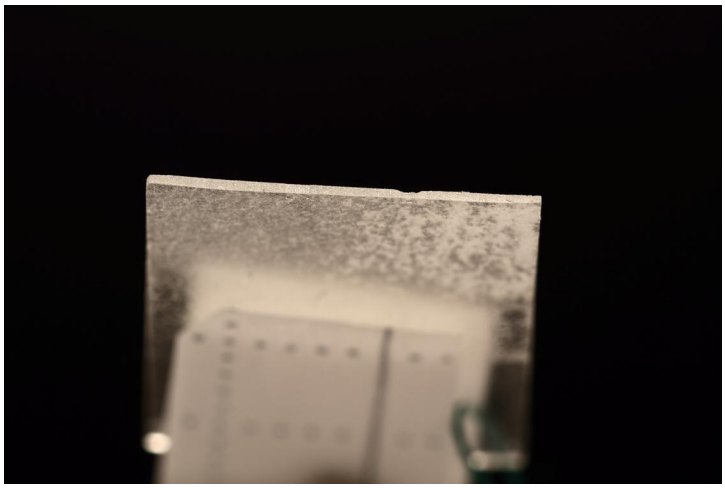

Figure 5.7 – Macroscopic picture of the leading edge of the Control group specimen after 30 min of solvent treatment, where only minor dissolution can be seen

5.1.2. Biomechanics

In figure 5.8 is presented the biomechanical testing results of the FRC material development study (I). Both the three point bending strength and Young's modulus showed that the developed material possesses similar characteristics to the human cortical bone. The plain PMMA implant showed inferior results in both. Human cortical bone values are presented here for comparison (Reilly and Burstein 1975, Lotz et al. 1991).

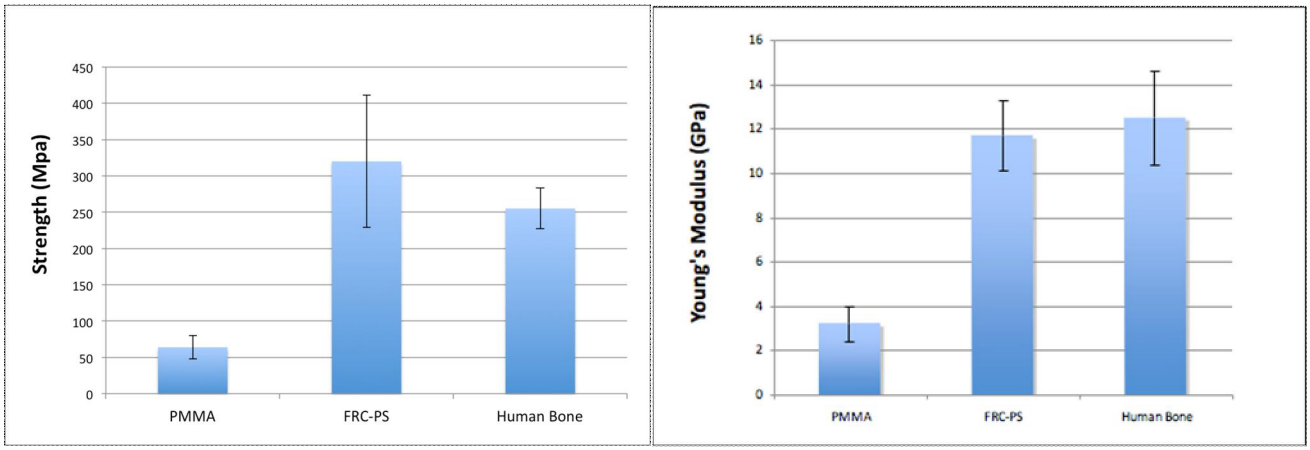

Figure 5.8 – Results of the biomechanical tests on FRC and PMMA, with a comparison to the properties of human cortical bone - according to Reilly and Burstein (1975) and Lotz et al. (1991)

5.1.3 – Experimental bone-bonding strength

The pullout testing was carried out with all of the specimens which retained their integrity after the solvent (THF) treatment. The detaching force varied greatly among the test groups, and a statistical analysis showed significantly higher forces for Group V at 5 minutes, compared to Group H (p=0.013) and Group R (p=0.019), and at 15 minutes for Group V compared to Group H (p=0,035). Figure 5.9.

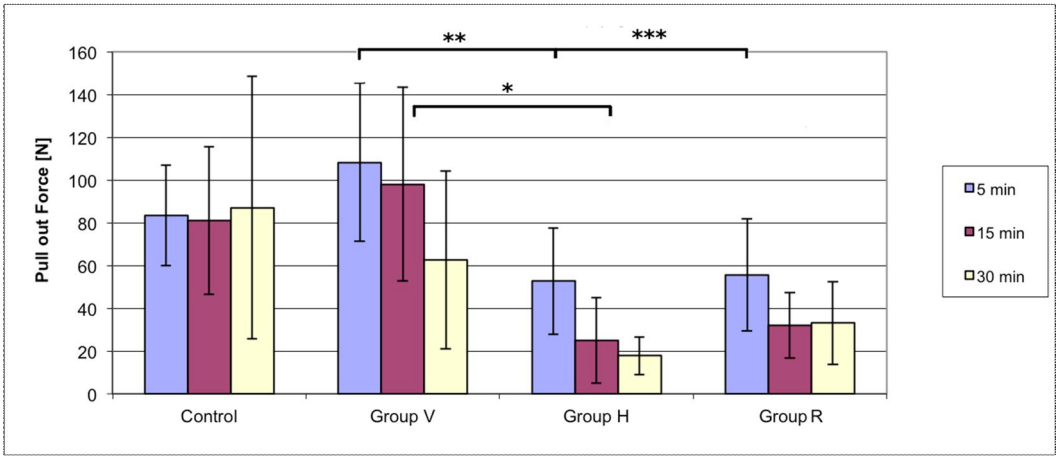

Figure 5.9 – Maximal pullout force of the composite specimens from the bone modeling material. Time-points refer to dissolving times of the samples (± 1 SD). Significant differences are marked with asterisks. (* - ***)

5.2. Cell cultures (study III)

5.2.1. – Soluble markers

Cell activity on the test specimens was related to the cell activity on the (non-toxic/neutral) control specimens (TCPS – tissue culture polystyrene) on day 1 which was set to represent 100% activity. All of the groups' cell activities increased during the study, but the R-PMMA was the only group to overcome the control specimens' activity significantly ($p<0.03$) on day 7. However this activity also declined rapidly after that, having the lowest activity at the end of the test. The cellular activity on the BG-PMMA specimens remained at a good level when compared to the control specimens throughout the study (no significant difference measured), indicating that the material was well tolerated.

The calcium concentrations declined in all of the cell culture mediums during the study period, which indicates that the cells on all test specimens had begun utilizing calcium. A Noteworthy observation was that the Ca-concentration in the BG-PMMA group increased significantly ($p< 0.001$) compared to all the other mediums in the beginning (on day 4), because of the release of Ca-ions from BG. The significantly lowest soluble calcium concentrations – suggesting the strongest utilization /mineralization /uptake of Ca-ions – was measured in the BG-PMMA group ($p<0.001$) on days 14 and 21.

A high BSP gene expression was measured in the cell stock in the beginning of the study, and after one week of culture, the BSP expression level had only slightly declined. No significant difference in BSP expression could be found between the groups during the study.

A low OC gene expression was measured ($\Delta CT = 0.2$) in the cell stock itself, but the activity increased (ΔCT ranged from 2.2 ± 0.1 to 5.0 ± 0.9) during the first week of culture. A significantly higher expression was measured fin the BG-PMMA and R-PMMA groups ($p=0.005$ and $p=0.012$ respectively) when compared to the TCPS on day 7. The highest OC expression was recorded in the BG-PMMA group - with a significant difference to the TCPS group ($p=0.015$) - on day 14. No statistically significant differences were measured between the S-PMMA, R-PMMA and BG-PMMA groups in either the BSP or the OC expression, which is mainly the result of large standard deviations within the groups.

The results of the cell culture studies are summarized in Figure 5.10

5.2.2. – Viability of cells

The first evaluation (day 1) revealed only some cell clusters on the surface of the specimens in all of the groups. At the second observation point (day 4) the R-PMMA and BG-PMMA groups showed emerging cell proliferation, as the cells spread over the surface and began to fill the grooves of the materials, while the S-PMMA group still had cells moving with pseudopodia extending out. By the day 7 pilkku the cells on the R-PMMA and BG-PMMA had covered the materials' grooves and calcifications (nodules) appearing on the surface, while S-PMMA showed no calcifications . All of the materials revealed a thick cell lining and a formation of calcification centers on day 14, and no new information was obtained from images on day 21 as the layer became thicker and the cells were buried deeper into the recesses of nodules.

SEM images from the cultured populations are summarized in Figure 5.11.

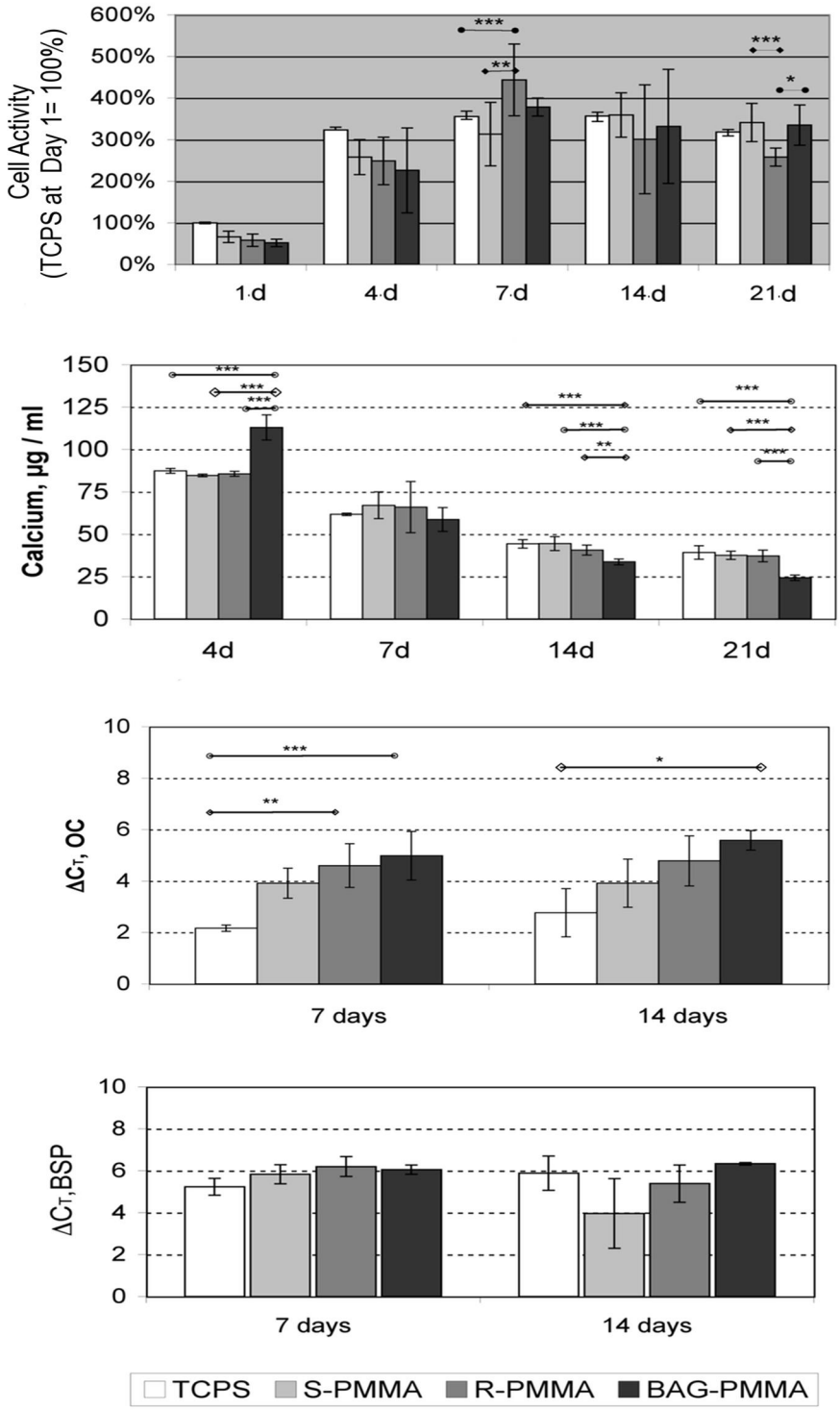

Figure 5.10. - Results of soluble markers analyzed from cell culture studies (★ - ★★★□- marking significant statistical difference)

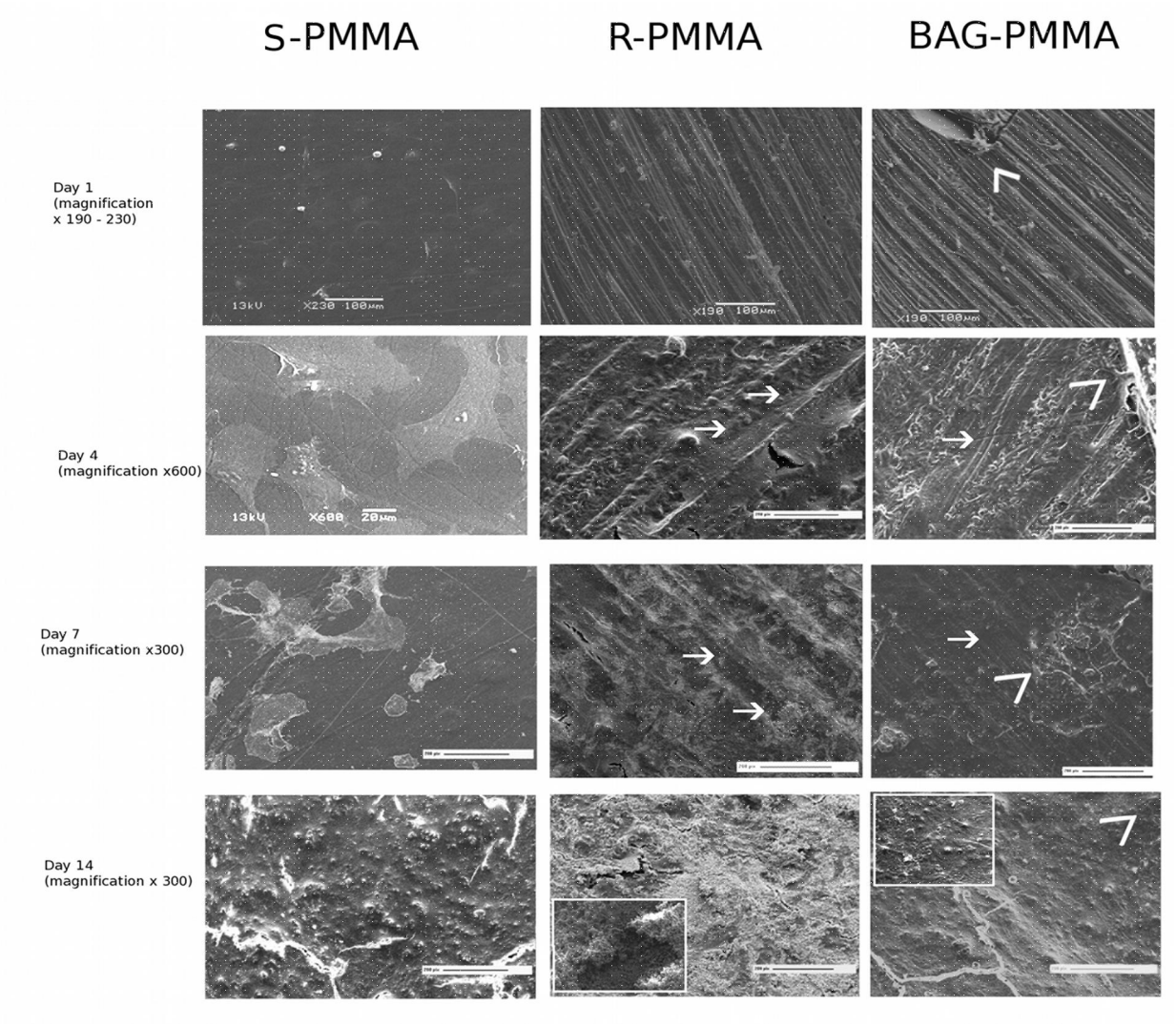

Figure 5.11 – SEM images of the cultured cell populations at different time-points

5.3. Animal experiments (study I and II)

The animals tolerated the surgical procedures well and no animal was lost during the surgery. Only one animal was lost during the follow-up (on day 3), as instability of the fixation was noted and the function of the limb was damaged. The animal was euthanized according to the study protocol and the guidelines of the Central Animal Laboratory. Other animals regained a good function of their limbs and were moving normally within days of surgery. They were in a good condition throughout the study (active, good appetite, no infections, etc.), as they were inspected daily by the personnel from the Animal Unit.

5.3.1. – Histological results

A Histological evaluation was conducted under a light microscope (magnification 2-40x), and possible gatherings of inflammatory cells (macrophages , lymphosytes etc.) were evaluated. No signs of infections or adverse foreign body reactions could be detected. New bone formation was already evident after 4 weeks of presenting, as trabecular bone was growing from the host periosteum junctions, and grew stronger by week 8, creating an external callus around the implant. Dense (lamellar) bone was seen in most specimens after 20 weeks, and intramedullary growth of bone could be detected in four out of nine (44%) FRC specimens at 20 weeks. A double cortex formation was detected on the posterior side of the implants (60%), where two perpendicular longitudinal lamellar bone bridges covered the length of the implant. In addition, bone marrow could be seen between these two bone layers. This is shown both on the radiographs and in the histological specimens (Figure 5.12). Some specimens displayed slight bone resorption at the junctions, which was suspected to be the result of an incomplete operational alignment between the sawed cortex and the end of the implant. This incongruence lead to a loading imbalance during weight bearing and to slight resorptive bone loss. Fibrous tissue was found intervening in some of the junction areas, predominantly in the misalignment group of specimens.

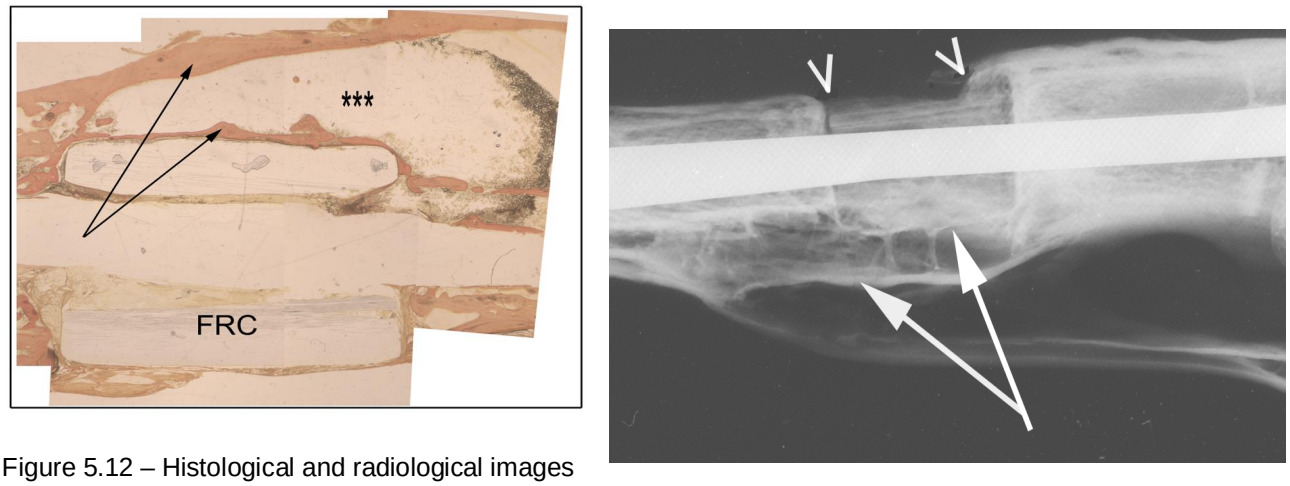

Figure 5.12 – Histological and radiological images displaying formation of lamellar bone and double cortex (arrows) and bone marrow (***)

5.3.2. – Histomorphometrical results

The posterior cortex bone contact index (BCI) was markedly higher for the FRC implant at 4 weeks (p=0.06) and significantly higher at 20 weeks (p=0.001), when compared to the control implant. These results were confirmed by an ANOVA test, which showed a clear group difference in favor of the FRC group, regardles of the follow-up time. In other measurement areas – anterior surface and intramedullary canal - the differences were not statistically significant. The total appositional bone growth (ABG) over the posterior side was of a higher degree in the FRC implant early in the study, but this was diminished by week 20. The BCI values of the measured junction area at 20 weeks revealed least bone contact in the FRC implant, which is believed to be due to the irregularity and uneven quality of the porous surface, which can lead to movement and fibrous tissue formation. The histomorphometrical results are presented in Table 5.1 and Figure 5.13.

Table 5.1 – Histomorphometrical data

		n	Average	SD	*p*
Total Appositional Bone Growth (Area%)					
4 wk					
	FRC	5	26.4	19.73	*0.19*
	Control	4	10.1	10.1	
8wk					
	FRC	4	37.6	9.09	*0.75*
	Control	4	32.1	35.7	
20wk					
	FRC	10	58.9	15.24	*0.68*
	Control	4	54.7	18.9	
Intramedullary Growth (Area %)					
4 wk					
	FRC	5	0	0	
	Control	4	0	0	
8wk					
	FRC	4	10.4	14.8	*0.758*
	Control	4	7.4	6.4	
20wk					
	FRC	10	18.3	30.4	*0.27*
	Control	4	25.2	23.6	
Posterior Surface BCI (%)					
4 wk					
	FRC	5	31.1	22.3	*0.058*
	Control	4	4.2	8.4	
8wk					
	FRC	4	38.6	27.5	*0.319*
	Control	4	7	6	
20wk					
	FRC	10	53.95	27.2	*0.014*
	Control	4	11.3	9.0	

		n	Average	SD	*p*
Anterior Surface BCI (%)					
4 wk					
	FRC	5	2.4	4.9	*0.44*
	Control	4	0	0	
8wk					
	FRC	4	4.7	9.4	*0.36*
	Control	4	0	0	
20wk					
	FRC	10	5.25	12.7	*0.42*
	Control	4	12.6	17.4	
Junction Area BCI (%)					
4 wk					
	FRC	5	3.4	3.3	*0.32*
	Control	4	10.1	14.1	
8wk					
	FRC	4	9.95	9	*0.99*
	Control	4	9.8	19.5	
20wk					
	FRC	10	9.8	7.8	*0.19*
	Control	4	17.6	11.9	
Porous surface growth (Area %)					
4 wk					
	FRC	5	17.8	13.6	
8wk					
	FRC	4	29.9	13	
20wk					
	FRC	10	40.7	25.3	

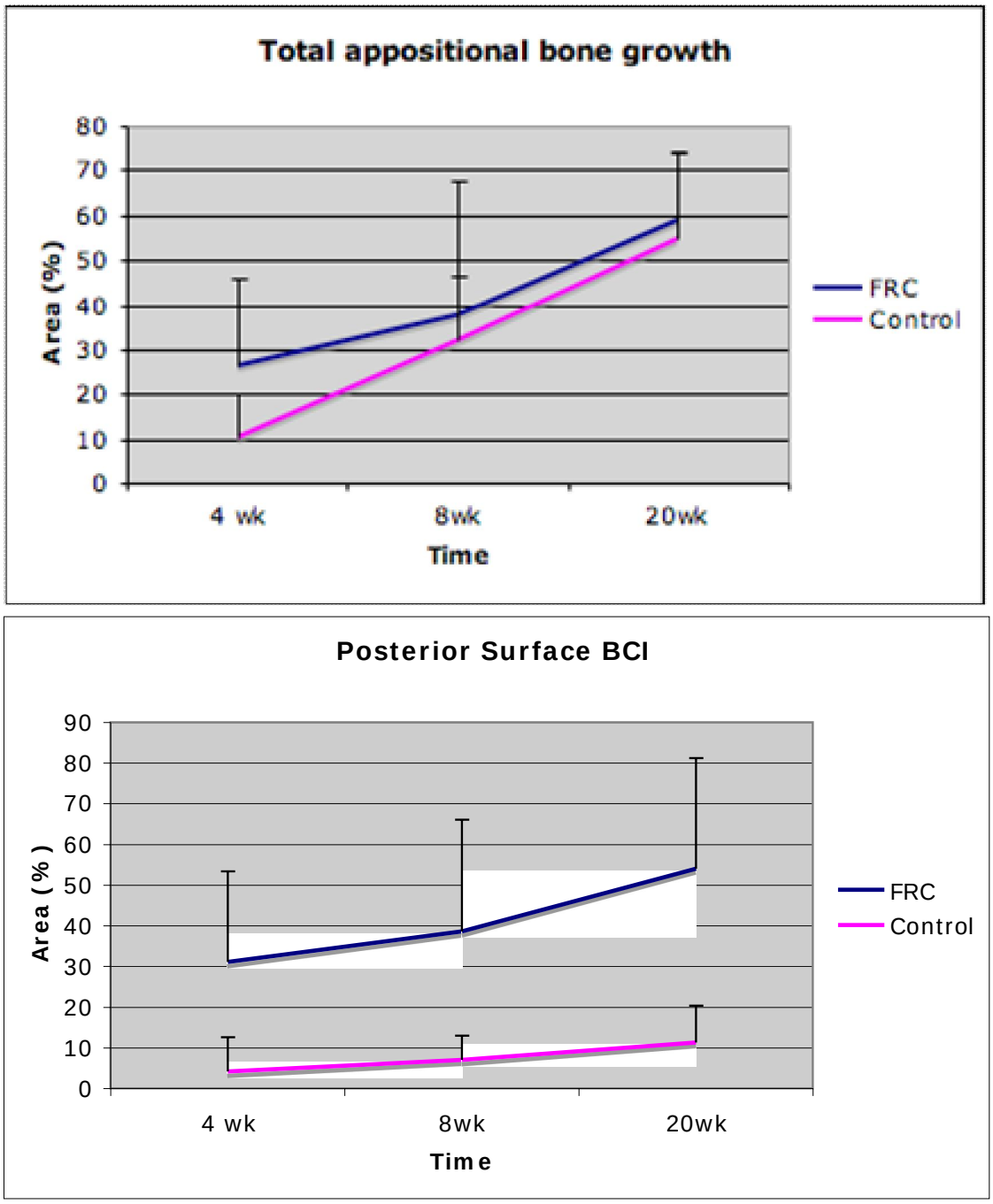

Figure 5.13 – Results of histomorphometry for Total appositional bone growth and Posterior surface BCI (whiskers represent SD)

5.3.3. – Radiological observations

Radiological images illustrate well the bone forming phenomena around the implant – a strong new bone callus covered the implant's sides as was confirmed in histological study. The anterior cortex showed less formation of new bone in all of the specimens, which was evident because it is the distraction

side of the tibia, as the compression created by weight bearing is exerted on the posterior aspect of the tibia. Some figures appeared to have formation of resorption of host bone at the ends of the implants (or clear space), but this was rather difficult to interpret reliably, because the PMMA itself is radiolucent and the only thing clearly visible in the X-ray is the fiber reinforcement. The anterior plating fixation method appered to be a more stable fixation as there was less callus formation at the posterior side of some of the implants as presented in Figure 5.14.

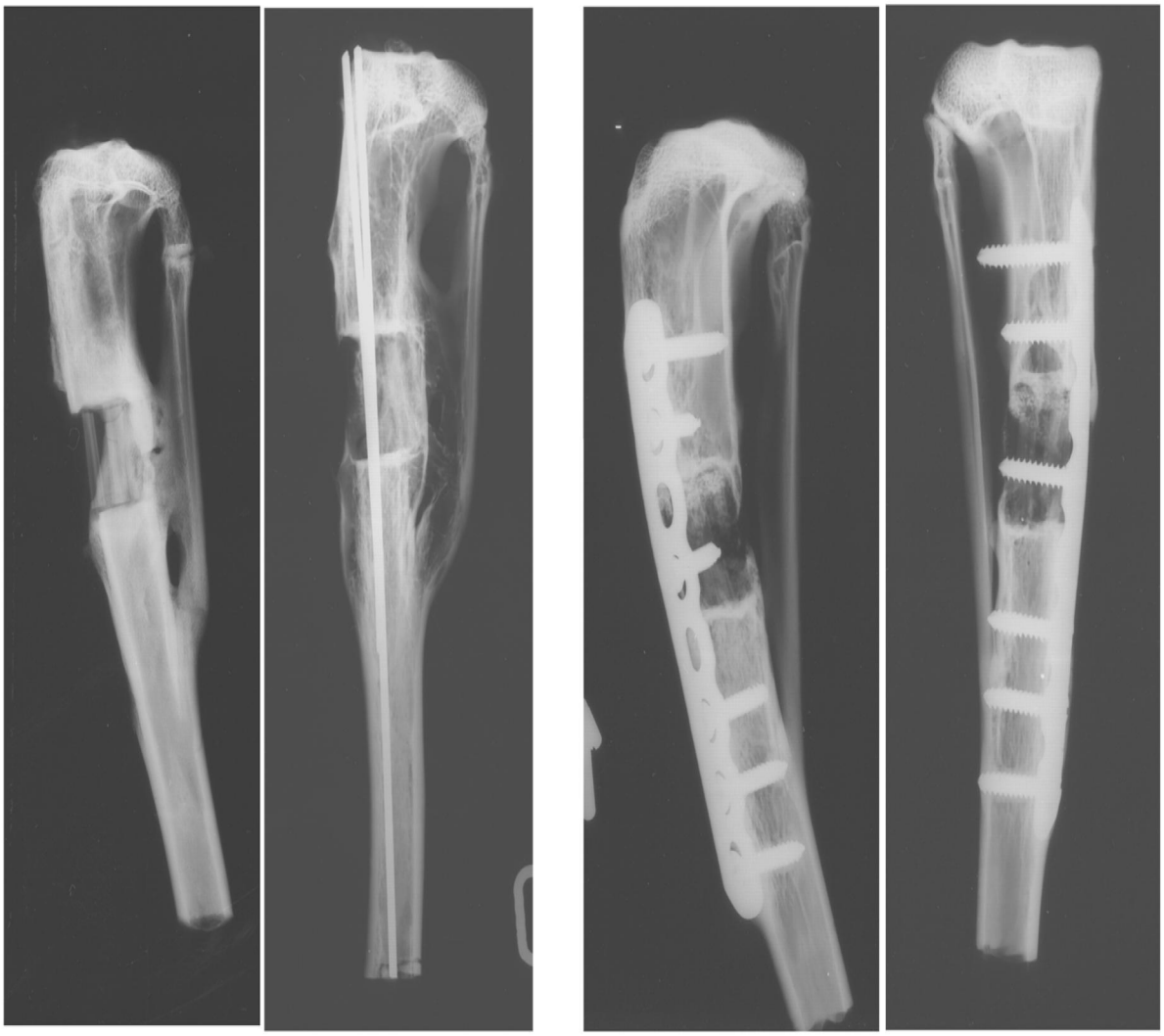

Figure 5.14 - Side views of the limbs after harvesting the tibias. Two different fixation methods show clear difference in the posterior callus formation (K –wires are removed from the first tibia on the left)

6 Discussion

6.1 - General Discussion

This study was initiated because there is a clinical need for relevant alternatives to large allografts and metal prostheses in the replacement of large segmental and weight-bearing bone defects. Problems with the use of large allografts are well documented, as are the long-term complications of metal prostheses used for limb salvage surgery (Thompson et al. 2000, Shin et al. 2000, Tanzer et al. 2003, Nishida et al. 2008). To address the stress shielding phenomena – a discrepancy in biomechanical properties, which leads to aseptic loosening and stress fractures - a lot of research has been done to create more flexible prostheses and fixation devices. Another problem with both the metal implants and allografts is the lack of incorporation to host bone. To enhance mechanical fixation and incorporation to host bone, a porous surface has been introduced to metal prostheses, and is applicaple to other materials as well (Hackin et al. 2003, Okada et al. 2008).

The use of PMMA in orthopaedics – mainly in joint replacement surgery - has continued since the 1950's as the primary fixation material for knee prostheses and in some hip replacements as well. The material has its drawbacks, but has prevailed in large-scale clinical use, even with some new augmentations to spinal and bone tumor surgery (Lewis 1997, Lieberman et al. 2005, Nishida et al. 2008). Bone cement (PMMA) has gone through many developments - additive filler materials, cross-linking agents, co-polymers, antibiotics, etc.- during these years, but still the most used form is a mixture of PMMA powder and MMA monomer liquid. It has proven to be the best alternative synthetic material to be used to fill bone defects, support osteoporotic bone and even act as a carrier of antibiotics in bone infections. In the resent decades, the use of fiber-reinforced PMMA cement has been introduced to medical applications, especially through extensive research in the field of dental and medical biomaterials. This has opened new possibilites for the use of PMMA in high-demand load-bearing applications.

In the current study, a new composite material was developed for bone replacement purposes. Porosity was created onto the surface of the implant with a new refined fabrication method, and it was done in an attempt to augment bone incorporation and mechanical interlocking. The characteristics of the material were tailored - while taking into consideration the weakening effect of the porosity to the structure of the implant - and biomechanically tested to meet the bone's properties.This study investigated the biological responses to the new composite material both *in vitro* and *in vivo* surroundings. The bone-bonding properties of the FRC material were also addressed in an experimental study design.

6.2 – Material development

The PMMA material was selected for this study because the material is non-bioresorbable (biostable), has relatively good strength retention in aqueous surroundings, and has long and wide-spread use in a clinical setting. (Lewis 1997, Vallittu 2007) The previous studies of PMMA – BG / HA composite implants have yielded promising results when repairing experimental bone defects in weight-bearing situations. Roughening the implant surface has proven to increase the bone's affinity to the material. (Heikkilä et al. 1997, Strandberg et al. 2001) To achieve the desired biomechanical properties for the implant, a longitudinal continuous fiber reinforcement was added into the core of the implant. Fiber reinforcement has been shown to increase the release of residual monomers and reagents from the material, but this can be diminished by a proper impregnation of the fibers by the resin component, the prepolymerization of the material and adequate water storage prior to use. (Vallittu 1995, Miettinen and Vallittu 1997).

E-glass fibers were chosen for the reinforcement, as they are well documented and found safe to be

used in medical composite materials (Vallittu 1999, Vallittu and Ekstrand 1999, Narva et al. 2005). It is known that the interfacial bonding of the fibers to the polymer matrix is crucial for the strength and durability of the implant, and thus silanized and preimpregnated fibers were used (Vallittu 1997 a, b). Despite the meticulous fabrication, there were still some difficulties at the early stages of the study in creating good quality specimens for the testing and implantation, due to the small size of the specimens. This could sometimes be seen as a non-uniform distribution of fibers in the implants or a minor quantity of fibers in specimens that were formed by cutting a larger block into smaller specimens. These could have contributed to some of the variance in the results which was noticed during the mechanical testing of the FRC specimens. In the future, the fabrication of larger specimens for the biomechanical testing could provide more standardized results. Methodologically, biaxial flexural testing should be considered as an alternative for the uniaxial three point bending tests to avoid an increased stress build-up on the edge of a small sized specimen (Palin et al. 2003).

The porous surface of the implants which were used in the present study for the animal testing was fabricated by partially dissolving the surface layer of the FRC core with a THF solvent. This created a foam-like PMMA with partially disentangled polymers, and as the solvent evaporated, the polymer foam solidified again. The evaporization of the THF left an open pore structure - with pore size ranging from 10 - 500 µm, confirmed by SEM (studies I and II) - which was suitable for bone ingrowth (Itälä et al. 2001). The surface structure was noted to vary in quality, as the implants were evaluated before surgery. Some of the porous surfaces were thin or did not even exist (bald spots), and therefore these specimens were discarded from the study and additionally analyzed by SEM (studies I and II). These findings lead to the further development of the manufacturing process, where the porous surface is created on the implants by changing the dissolving time and fiber orientation of the FRC core (study IV). Performing in vitro fatigue testing on the material in the future could provide even more information about the strength of the fiber-reinforced porous surface structure created by the dissolution process.

6.3 – Animal experiments

Animal experiments are an important step in developing a new medical device or material for human applications. A good animal model can display the drawbacks of a technique or material and minimize the risks before advancing to human testing, but no animal test result (biocompatibility, durability or biomechanical strength) can be directly applied to humans. Choosing a suitable animal for a bone segment defect model is a demanding task. The closest resemblances to humans in respect to body mass and cortex ratio are sheep or pigs, but canines and rabbits are often used as well. Larger animals, such as sheep or pigs, present a similar axial loading pattern on the tibia as humans, and their activity type and level are similar – mainly walking or standing. Dogs and rabbits present higher speed / acceleration while moving (jumping or running), which creates higher biomechanical stress (bending /shearing) on their limbs, providing information about the fatigue resistance / durability of the material. Rodents (mice, rats, etc.) have a very high activity level, and thus present greater stress to their body, but they possess a higher speed of bone and soft tissue t turnover , and their lifespan is also much shorter. The small size of rodents makes the fixation of segment defects unreliable. (Reichert et al. 2009)

Rabbits reach maturity quickly (within 6 months), are easily maintained, and accomodate well to single housing. Our laboratory’s previous good experiences with New Zealand White rabbits was also a decisive factor in the matter. The cross-sectional shape of the tibia in a rabbit's body is rounded trigonal. The cortexes are rather thin - but durable, not brittle - and possess a large medullary cavity to house intramedullary devices. These facts made rabbits a good subject for a segment defect model. Although the stance and gait of the animal differed from that of humans, there is axial loading on the tibia. A rabbit's fibula is united with the mid portion of the tibia (posteriorly) – differing from human tibias. The fibular bone is very thin and does not carry (axial) weight, but may give support against rotational forces in a segmental defect model, when a part of the tibia is excised. The radiographs taken during the study revealed that the fibula had been fractured in some of the animals, and either

was healed or in the process of healing with a strong callus. This callus appeared in the radiographs to be attached to the posterior callus formation of the segment defect, but no bone attachment was found as the specimens were prepared for histological processing where the fibula needed to be removed.

Due to the more flexed position of the knee, there is more tension on the anterior cortex of the rabbit tibia and compression on the posterior side than in human counterparts. This could be seen as favorable for the anterior plating technique, where the plate acted as a compression device resisting the tension and anterior buckling of the construct. Intramedullary nailing has been considered a more rigid fixation for diaphyseal fractures as it fills the intramedullary cavity, thus resisting bending and torsional forces better (closer to the midline, no directional difference, etc.). The use of three K-wires placed tightly (with the use of a hammer) to fill the intramedullary cavity of rabbit tibia corresponds to (non-locking) intramedullary nailing.

No difference could be detected in bone healing between the two fixation methods used in this study. This finding was in agreement with the work of Benevenia et al. (2000), where canine segment defects were fixed with either intramedullary nailing or plate fixation. This finding can be explained through the intricate balance between the required stability and beneficial motion affecting the healing of bone damage. Many studies investigating fracture or osteotomy healing have shown that, although stability is important for healing, straining the repairing bone tissue within certain intervals is beneficial for healing, and too rigid a fixation can lead to weakening of the bone around the implant (e.g. decreased vascular supply and stress shielding). (Ulstrup 2008, Shapiro 2008)

During surgery, the segment defect was created by a hand-held, water-cooled circular saw. This lead to minor differences in the length of the segment defect, and exact parallel cuts could not always be established. However, the implants could easily be adjusted to the exact length of the defect by slightly grinding the ends of the implant. The implant was gently pushed onto the defect and a tight fit, a so-called press fit, was established before the application of the fixation. The outer radius of the implant and host bone did not match exactly, but the thickness of the wall of the tubular implant provided tolerance for the minor discrepancies.

6.4 - Histology

The samples for the histological examination were prepared as non-decalcified samples, which meant that the exiced samples of tibia, 2-3 cm in length, containing the implant were embedded into acrylic resin. The embedded samples were then prepared with a cutting-and-grinding technique to the final microscope slides and stained with the Masson-trichrome and van Gieson methods. To prevent the samples from tearing apart during the grinding process, the thickness of the samples was left rather large. This caused difficulties in the interpretation of the Masson-stained samples as they were intensively coloured and appeared dark when inspected, which made it difficult to distinguish whether or not the interface between the bone and the implant had any fibrous tissue. This impaired the computer-assisted histomorphometric (BCI) measurements, and therefore the measurements were only done on the van Gieson stained specimens.

Histological examination showed strong new bone formation on the posterior aspect of the implant, which
has also been demonstrated to occur in large osteoarticular allografts in humans evaluated by CT-scanning. This was thought by Mattila and coworkers (1995) to be a biomechanical response to loading. A thick new trabecular bone formation over the FRC implants was noted during the study. This was thought to be due to the porous surface layer, because it has not been observed in large segmental allografts with smooth surfaces (Aho et al. 1996, Enneking and Campanacci 2001). Generally considering, the incorporation model of the FRC-implant - the bridging bone growth, the external callus over the junction areas and the appositional surface bone growth - resembles the repair of a large structural human allograft, porous surface tumor prostheses, and experimental segment repair in animals. (Okada et al. 1988, Delloye et al. 1990, Benevenia et al. 2000, Enneking and Campanacci 2001, Tanzer et al. 2003)

The bone contact index (BCI) was used to determine the amount of bone in direct contact with the implant and it corresponds to the affinity index (AI) reported previously by Schizato et al. (2001). The BCI has been reported to correlate well with evaluations taken from microradiographs of the interface area (Mattila 2009).

The low BCI values at the junction areas were thought to be due to an improper fit between the implant interface and the cortex, and insufficient compression and stability at the bone-implant interface. The irregularity of the porosity and possible weakness of the porous surface might allow the surface layer to be compressed under the load, causing loss of stability. These could have caused micromotion during gait, and lead to the formation of fibrous tissue and non-union. The weakness of the porous surface layer could be due to the fact that the fibers of the FRC were not protruding to the porous surface layer; instead they were limited only to the core. The porous surface layer was noted detaching from some of the samples prior to implantation. This inherent weakness may also be debated to have caused later shedding of PMMA particles from the porous surface, and thus irritation in the surrounding tissues, leading to aseptic loosening of the implant. This theory is in contradiction with the finding that no foreign body (macrophages) reactions could be seen around the implants.

The least amount of new bone formation was measured at the anterior side of the implant in both the FRC and control implants. The anterior placement of the fixation plate was a possible factor interfering (stress shielding) the bone formation anteriorly, but this explanation was not supported by the fact that intramedullary nailing did not provide any more bone formation anteriorly.

6.5 – Cell Culture

Cell proliferation studies were done on disk-shaped specimens, which were suitable for tissue culture chambers. The specimens were fabricated from the same materials as the FRC implants, but the creation of porous surface was limited to surface roughening due to the small size of the specimens. Moreover, the formation of porosity onto the cell culture disks would have caused the cells to fall into the pores. This would have made it difficult or even impossible to visualize the early growth and attachment of the osteoblast cells. The fiber reinforcement is not present in the cell culture discs, as they were left out in an attempt to maximize the amount of BG on the surface of the small disks, which were fabricated from larger cylinders as described earlier. The lack of fiber was evaluated to have a minimal effect, as the E-glass is considered non-toxic and inert in normal SBF surroundings. The presence of the fibers could have provided more incongruences in the material, thus affecting the properties of the surface of the disc.
All of the soluble markers that were tested indicated good cellular activity and viability of the osteoblasts on all of the test materials. Cellular functions on the rough surface and bioactive glass containing specimens were significantly enhanced in relation to OC and BSP secretion, which have been related to good biocompatibility through normal maturation and function of osteoblasts (Cooper et al. 1998, Ohsawa et al. 2001). The concentration of Ca-ions in the culture medium was significantly lower for the BG group at the end of the study, which can be interpreted as good uptake and deposition by differentiated, viable and active cells (Donzelli et al. 2007). SEM imaging provided support for these findings as the rough surface and BG elicited the fastest division of cells and an early production of calcium precipitates onto the samples. This is in concurrence with previous reports of the effects of microrough surfaces and bioactive glass (Itälä et al. 2002, Hacking et al. 2003, Välimäki and Aro 2006).

6.6 – Fiber orientation and bone-bonding ability

As the porous surface structure made by the dissolving process was found unsatisfactory regarding the compressive strength and uniformity of the material, an enhancement to the process was developed, and took advantage of the fiber reinforcement aiding the dissolution of the surface. This provided a basis for a test comparing the effects of different dissolving times and fiber-reinforcement orientations on the bone-bonding ability of the material. Specimens were fabricated for this study using only PMMA and E-glass fibers, because the BG would have provided an additional confounding factor to the analysis as the strength of small specimens could have been affected by addition of particulate BG. The specimen size was adjusted according to the previous experiences of Mattila et al. (2004), as the larger specimens suffered from slow dissolving speeds.

The fiber reinforcement in the PMMA matrix increased the solubility of the material substantially, regardless of the direction of the fibers, when compared to non-fiber-reinforced PMMA specimens. The fastest dissolving speed was noted in the group V, where the fibers were aligned longitudinally to the long axis of the specimen, which helped the penetration of solvent into the polymer matrix by a capillary effect created by micro gaps between the fibers and polymer matrix. This could have led to an easier penetration of solvent into the polymer matrix and the disentanglement of the polymer chains. The Diffusion of dissolved loose polymer chains out from the polymer matrix could, in turn, occur easier through the minor gaps close to the fibers. In addition, cracking and crazing of the polymer matrix of the FRC specimens at the early stage of the solvent treatment suggested rapid penetration of solvent causing an increase in the internal pressure of the polymer matrix (Miller-Chou and Koenig 2003).

The assumptions of the capillary effects of the reinforcing fibers are somewhat in conflict with some of the previous studies on particulate-reinforced polymers, where the (solid, non-absorbing) filler material decreased the wettability and swelling of the material, which are considered crucial for the dissolving phenomena (Burnside and Gianellis 1995, Thomason and Porteus 2011). Moreover, the silane treatment and pre-wetting of the fibers with monomers should increase the bonding between the matrix and fibers, thus lowering the progression of solution (Park and Jin 2001, Debnath et al. 2003). The other consideration is the fact that the fibers in FRC specimens reduce the total volume of the polymer matrix and thus the absolute volume of PMMA to be dissolved is less than in the specimens made only of PMMA, i.e. without fibers. This relationship to fiber volume content remains to be studied further.

The use of bone-simulating materials in a preliminary evaluation of the biomechanical properties of medical devices is not uncommon. They do not replace the use of animal bone or cadaver bone, or in vivo testing of fixation devices, but there are many advantages in the use of artificial materials: a consistent size, shape and density, and they can also be modeled to nearly any form. As the material's properties are constant, a reliable reproduction of test conditions is possible, thus yielding constant results. Materials with a similar density, compressive strength and microporosity – such as low-density polyurethane, wood and PMMA - have been used in experiments when testing the bone-bonding abilities of different fixation or anchoring devices (Berzins et al. 1997, Nien et al. 2001, Ricalde et al. 2005, Bailey et al. 2006, Zdero et al. 2007, Buijs et al. 2007). Pullout testing with the use of dental stone as a material simulating bone bonding has not been validated. Dental stone has been reported to have similar biomechanical properties – the modulus approximately 10 GPa and compressive strength approximately 40-50 MPa - to human cancellous bone (Rho 1997, Lotz et al. 1991, Bayraktar et al. 2004, Kim et al. 2006). Dental rock has previously been used when testing the bone-bonding capabilities of bone replacement materials or fixation devices, with good reproducibility (Mattila et al. 2006, Ballo et al. 2007, Nganga et al. 2011).

The increase in the pullout strength of the fiber-reinforced specimens was hypothesized to occur because the increased number of fibers, which were protruding from the surface, would enlarge the surface area of the composite material. With dissolution times of 5 and 15 minutes, Group V

(longitudinally exposed fibers) provided better bonding properties and higher detachment forces than the other groups. However, when prolonging the dissolving period, the detachment forces decreased in all of the fiber-reinforced specimens below the values of the control group. After 30 minutes of dissolution, the FRC specimens had only fibers protruding from the surface, and as the matrix was completely dissolved, it did not provide any structural support. This produced some difficulties in testing the FRC specimens, because they had become fragile and difficult to handle. The control specimens did not show marked reduction in size or consistency, and thus, the strength of the matrix was retained.

The homogeneity of all the FRC specimens was extensively deteriorated by the last time-point, and the reinforcing fibers already detaching from the surface. This could prove a noteworthy observation, when considering the design of future implants made with non-continuous fiber reinforcement, as these fibers might be shed off the surface, increasing particulate debris (fibers, PMMA) in the tissues surrounding the implant.

7 – Conclusions

Based on the studies included in this thesis, the following conclusions can be made

I It is possible to manufacture a fiber-reinforced PMMA-based implant with surface porosity suitable for bone ingrowth. The biomechanical properties can be tailored with fiber reinforcement to match the cortical bone. The Implants tolerated the load-bearing surroundings of a segment defect model in rabbits well.

II The FRC implant worked well in repairing the segment defect in a long-term evaluation. No adverse or toxic reactions could be seen in either of the pre-fabricated materials implanted into test animals. The FRC implant proved superior to the control material in conducting new bone growth onto and along the porous surface when evaluated by the BCI method.

III The test materials showed good biocompatibility in cell culture tests. The cell divisions or cellular functions were not attenuated when planted onto the test materials, but rather increased when compared with cells planted onto the control materials.

IV The fiber reinforcement significantly increased the solubility of the matrix PMMA of the specimens and the orientation of the reinforcing fibers had a profound effect on the process of exposing fibers for the bone attachment. Short solvent treatment times increased the bonding strength of the FRC material to simulating bone and longer treatment times had a deleterious effect on the homogeneity of the implant material.

8 - Future propects

Fiber-reinforced composites have proven versatile and easily adapted to meet the different biomechanical requirements of medical implants and devices. As an implant material, they are durable enough to withstand cycling loading by the host animal or patient.

The beneficial effects of surface porosity and exposed glass on bone growth seem to be obvious. Investigating the creation of porosity by altering the fiber orientation was the first step in the process of understanding the complex dissolution mechanisms of the FRC's. The effect of different fiber proportions and mixing different fiber lengths and orientation could be explored in the future. By optimizing the specimens' size for the solvent treatment could also provide insight into the kinetics of the solution process to further improve the quality of the surface of the implant. An alternative approach to using FRC is based on using thermosetting resins instead of thermoplastic PMMA. An Example of a biocompatible thermoset is bisphenol-A-glycidyl methacrylate (bisGMA), which has been used succesfully in cranial implants. Further development of thermoset resin implants by porous surface structure established in this study is to be done in the future.

Safety issues are important with biomaterials and medical devices. All new materials and material combinations need to be carefully tested in terms of biocompatibility pilkku and risk analysis related to the materials has to be carried out before proceeding to the clinical testing of the materials.

ACKNOWLEDGEMENTS

This research was carried out in collaboration of the Department of Prosthetic Dentistry and Biomaterials Research and the Department of Orthopaedics and Traumatology at the University of Turku during the years of 2000 – 2012. The study was begun as a part of the POTRA (polymers for building the future) project by TEKES (the Finnish Funding Agency for Technology and Innovation) and it was continued at the Turku Clinical Biomaterials Center in the FRC Research Group.

First I'd like to extend my warmest gratitude to my senior supervisor professor Allan Aho, who is the true farther and mastermind behind the bone defect repair study. From the beginning of the study he has been guiding and supporting me from the first baby steps of animal surgery and histological analysis to bold stride of a young scientist confident of his ability – and ever so carefully reminding about the facts of life and limitations of our knowledge. His endless enthusiasm and energy for research, ability to think ”out of the box” and come up with new ideas is inspiration for all young minds.

I'm also forever grateful to my other supervisors professor Pekka Vallittu (who continued after the retirement of professor Antti Yli-Urpo) and adjunct professor Mervi Puska. Professor Vallittu has made this study possible by enabling it to continue under the FRC Reserach Group, despite the long absences of the primary researcher. His encouraging advice and relentless - but warm - guidance has been crucial in the finishing stages of this thesis project. Adjunct professor Puska has offered me countless hours of her time both in- and outside of the laboratory – whether she is in Turku, Espoo or Oslo – and not always without nuisance and personal sacrifice. Without her work the final study could still be in the process of making. She has also proven to be the voice of reason when our ideas have been too far reaching.

The other collaborators of this research are equally appreciated. Jami Rekola and Jarmo Gunn with whom we performed all of the animal surgeries and histological preparations - we were never bored. Pasi Alander offered his knowledge and skill in manufacturing of the implants, and was never too busy to help me. Riina Mattila helped tremendously in the development of the implant and assisted in the odd-jobbs when I happened to appear in Turku. Ville Meretoja performed the cell cultures and offered invaluable advice on the statistical analysis. Teemu Tirri is a magician when it comes to electronic devices – whether it is a SEM microscope or a computer assisted histometer - and he is another voice of reason amongst us. Esko Lahtinen has offered his expertice in many of the illustrations used for this study. My sincere thanks go to the personel of Institute of Denstistry and FRC Research Group, especially Annikki Väistö, Tarja Peltoniemi and Päivi Mäki who have helped me tremendously.

I am deeply grateful to the reviewers of this thesis, professor Nils Gjerdet and professor Reijo Lappalainen. Your exellent comments and suggestions made this thesis much better.

I want to thank TEKES, University of Turku Foundation - Allan Aho Fund, HUCH /EVO-funding and SOT – Research Foundation for financial support of this work.

My dear old friends since childhood - the life before medicine – deserve a special thanks. They've kept me in connection with the real word. Especially the yearly fishing trips to the beautiful Finnish Archipelago have offered a much needed break from the routines.

Last but not least I wish to thank my family for the love and support during these years, and appologise for all the inconvenience I have caused with my ”absence”.

Espoo, November 2012

Mikko Hautamäki

REFERENCES

Abu Bakar, M. S., Cheng, M. H., Tang, S. M., Yu, S. C., Liao, K., Tan, C. T., et al. (2003). Tensile properties, tension-tension fatigue and biological response of polyetheretherketone-hydroxyapatite composites for load-bearing orthopedic implants. *Biomaterials, 24*(13), 2245-2250.

Aho, A. J., Ekfors, T., Knuuti, J., Mattila, K., & Heikkilä, J. (1996). Repair of massive allografts: Histological, nuclear medicine and CT-studies. In A. A. Czitstrom, & K. H. Winkler (Eds.), *Orthopaedic allograft surgery* [Repair of massive allografts: histological,, nuclear medicine and CT-studies] (pp. 67--73). Austria: Springer-Verlag.

Aho, A. J. (1966). Electron microscopic and histological observations on fracture repair in young and old rats. University of Turku).

Aho, A. J., Eskola, J., Ekfors, T., Manner, I., Kouri, T., & Hollmen, T. (1998). Immune responses and clinical outcome of massive human osteoarticular allografts. *Clinical Orthopaedics and Related Research, (346)*(346), 196-206.

Aho, A. J., Hautamaki, M., Mattila, R., Alander, P., Strandberg, N., Rekola, J., et al. (2004). Surface porous fibre-reinforced composite bulk bone substitute. *Cell & Tissue Banking, 5*(4), 213-221.

Ai-Aql, Z. S., Alagl, A. S., Graves, D. T., Gerstenfeld, L. C., & Einhorn, T. A. (2008). Molecular mechanisms controlling bone formation during fracture healing and distraction osteogenesis. *Journal of Dental Research, 87*(2), 107-118.

Bailey, C. A., Kuiper, J. H., & Kelly, C. P. (2006). Biomechanical evaluation of a new composite bioresorbable screw. *Journal of Hand Surgery - British Volume, 31*(2), 208-212.

Ballo, A. M., Akca, E. A., Ozen, T., Lassila, L., Vallittu, P. K., & Narhi, T. O. (2009). Bone tissue responses to glass fiber-reinforced composite implants--a histomorphometric study. *Clinical Oral Implants Research, 20*(6), 608-615.

Ballo, A. M., Lassila, L. V., Vallittu, P. K., & Narhi, T. O. (2007). Load bearing capacity of bone anchored fiber-reinforced composite device. *Journal of Materials Science-Materials in Medicine, 18*(10), 2025-2031.

Ballo, A. M., Narhi, T. O., Akca, E. A., Ozen, T., Syrjanen, S. M., Lassila, L. V., et al. (2011). Prepolymerized vs. in situ-polymerized fiber-reinforced composite implants--a pilot study. *Journal of Dental Research, 90*(2), 263-267.

Barak, M. M., Lieberman, D. E., & Hublin, J. (2011). A wolff in sheep's clothing: Trabecular bone adaptation in response to changes in joint loading orientation. *Bone, 49*(6), 1141-1151.

Barton, A. (1985). Aplications of solubility parameters and other cohesion parameters in polymer science and technology. *Pure and Applied Chemistry, 57*(7), 905-912.

Basant, G., & Reddy, Y. G. (2011). The effect of incorporation, orientation and silane treatment of glass fibers on the fracture resistance of interim fixed partial dentures. *The Journal of Indian Prosthodontic Society, 11*(1), 45-51.

Bayraktar, H. H., Morgan, E. F., Niebur, G. L., Morris, G. E., Wong, E. K., & Keaveny, T. M. (2004). Comparison of the elastic and yield properties of human femoral trabecular and cortical bone tissue. *Journal of Biomechanics, 37*(1), 27-35.

Benevenia, J., Zimmerman, M., Keating, J., Cyran, F., Blacksin, M., & Parsons, J. R. (2000). Mechanical environment affects allograft incorporation. *Journal of Biomedical Materials Research, 53*(1), 67-72.

Berzins, A., Shah, B., Weinans, H., & Sumner, D. R. (1997). Nondestructive measurements of implant-bone interface shear modulus and effects of implant geometry in pull-out tests. *Journal of Biomedical Materials Research, 34*(3), 337-340.

Bobyn, J. D., Stackpool, G. J., Hacking, S. A., Tanzer, M., & Krygier, J. J. (1999). Characteristics of bone ingrowth and interface mechanics of a new porous tantalum biomaterial. *The Journal of Bone and Joint Surgery. 81 B*(5), 907-914.

Boesel, L. F., Azevedo, H. S., & Reis, R. L. (2006). Incorporation of alpha-amylase enzyme and a bioactive filler into hydrophilic, partially degradable, and bioactive cements (HDBCs) as a new approach to tailor simultaneously their degradation and bioactive behavior. *Biomacromolecules, 7*(9), 2600-2609.

Bonfield, W. (1988). Hydroxyapatite-reinforced polyethylene as an analogous material for bone replacement. *Annals of the New York Academy of Sciences, 523*, 173-177.

Boyan, B. D., Hummert, T. W., Dean, D. D., & Schwartz, Z. (1996). Role of material surfaces in regulating bone and cartilage cell response. *Biomaterials, 17*(2), 137-146.

Bruder, S. P., Kraus, K. H., Goldberg, V. M., & Kadiyala, S. (1998). The effect of implants loaded with autologous mesenchymal stem cells on the healing of canine segmental bone defects. *Journal of Bone & Joint Surgery, 80 A*(7), 985-996.

Bruens, M. L., Pieterman, H., de Wijn, J. R., & Vaandrager, J. M. (2003). Porous polymethylmethacrylate as bone substitute in the craniofacial area. *Journal of Craniofacial Surgery, 14*(1), 63-68.

Buijs, G. J., van der Houwen, E. B., Stegenga, B., Bos, R. R., & Verkerke, G. J. (2007). Mechanical strength and stiffness of biodegradable and titanium osteofixation systems. *Journal of Oral & Maxillofacial Surgery, 65*(11), 2148-2158.

Burnside SD, & Giannelis EP. (1995). *Synthesis and properties of new poly(dimethylsiloxane) nanocomposites* - American Chemical Society.

Burr, D. B. (2011). Why bones bend but don't break. *Journal of Musculoskeletal Neuronal Interactions, 11*(4), 270-285.

Cao, W., & Hench, L. L. (1996). Bioactive materials. *Ceramics International, 22*(6), 493-507.

Chao, E. Y., S, Inoue, N. E.,John J., & Aro, H. (1998). Enhancement of fracture healing by mechanical and surgical intervention. *Clinical Orthopaedics & Related Research.Fracture Healing Enhancement, 355*(Supplement), S163-S178.

Charnley John. (1960). Anchorage of the femoral head prosthesis to the shaft of the femur *Journal of Bone and Joint Surgery-British Volume, 42 B*(1), 28--30.

Chevalier, E., Chulia, D., Pouget, C., & Viana, M. (2008). Fabrication of porous substrates: A review of processes using pore forming agents in the biomaterial field. *Journal of Pharmaceutical Sciences, 97*(3), 1135-1154.

Cooper, L. F., Yliheikkila, P. K., Felton, D. A., & Whitson, S. W. (1998). Spatiotemporal assessment of fetal bovine osteoblast culture differentiation indicates a role for BSP in promoting differentiation. *Journal of Bone & Mineral Research, 13*(4), 620-632.

Dean, D. P. D., Topham, N. S. M. D., Rimnac, C. P. D., Mikos, A. G. P. D., Goldberg, D. P. M. D., Jepsen, K. P. D., et al. (1999). Osseointegration of preformed polymethylmethacrylate craniofacial prostheses coated with bone marrow-

impregnated poly (DL-lactic-co-glycolic acid) foam. *Plastic & Reconstructive Surgery, 104*(3), 705-712.

Debnath, S., Wunder, S. L., McCool, J. I., & Baran, G. R. (2003). Silane treatment effects on glass/resin interfacial shear strengths. *Dental Materials, 19*(5), 441-448.

Delloye, C., Delefortrie, G., Coutelier, L., & Vincent, A. (1990). Bone regenerate formation in cortical bone during distraction lengthening. an experimental study. *Clinical Orthopaedics and Related Research,* (250), 34-42.

Demir, H., Dogan, O. M., & Dogan, A. (2012). Tensile properties of denture base resin reinforced with various esthetic fibers. *Journal of Applied Polymer Science, 123*(6), 3354-3362.

den Boer, F. C., Wippermann, B. W., Blokhuis, T. J., Patka, P., Bakker, F. C., & Haarman, H. J. (2003). Healing of segmental bone defects with granular porous hydroxyapatite augmented with recombinant human osteogenic protein-1 or autologous bone marrow. *Journal of Orthopaedic Research, 21*(3), 521-528.

Dietz, F. R., & Morcuende, J. A. (2006). BONE FORMATION AND GROWTH. In R. T. Morrissy, & S. L. Weinstein (Eds.), *Lovell & winter's pediatric orthopaedics* (6th ed.). 530 Walnut Street, Philadelphia, PA 19106 USA: Lippincott Williams & Wilkins.

Dimitriou, R., Tsiridis, E., & Giannoudis, P. V. (2005). Current concepts of molecular aspects of bone healing. *Injury, 36*(12), 1392-1404.

Donzelli, E., Salvade, A., Mimo, P., Vigano, M., Morrone, M., Papagna, R., et al. (2007). Mesenchymal stem cells cultured on a collagen scaffold: In vitro osteogenic differentiation. *Archives of Oral Biology, 52*(1), 64-73.

Dyer,S.R., Lassila,L.V., Jokinen,M., Vallittu, P.K. (2005). Effect of cross-sectional design on the modulus of elasticity and toughness of fiber-reinforced composite materials. *The Journal of prosthetic dentistry*,94(3), 219-226

Einhorn, T. A. (1995). Enhancement of fr.acture-healing. *Journal of Bone & Joint Surgery, 77 A*(6), 940-956.

Engh, C. A., Bobyn, J. D., & Glassman, A. H. (1987). Porous-coated hip replacement. the factors governing bone ingrowth, stress shielding, and clinical results. *Journal of Bone & Joint Surgery, 69 B*(1), 45-55.

Enneking, W., Eady, J., & Burchardt, J. (1980). Autogenous cortical bone grafts in the reconstruction of segmental skeletal defects. *Journal of Bone & Joint Surgery, 62 A*, 1039-1058.

Enneking, W. F., & Campanacci, D. A. (2001). Retrieved human allografts : A clinicopathological study. *The Journal of Bone and Joint Surgery, 83 A*(7), 971-986.

Eppley, B. L., Pietrzak, W. S., & Blanton, M. W. (2005). Allograft and alloplastic bone substitutes: A review of science and technology for the craniomaxillofacial surgeon. *Journal of Craniofacial Surgery, 16*(6), 981-989.

Eward, W. C., Kontogeorgakos, V., Levin, L. S., & Brigman, B. E. (2010). Free vascularized fibular graft reconstruction of large skeletal defects after tumor resection. *Clinical Orthopaedics & Related Research, 468*(2), 590-598.

Finkemeier, C. G. (2002). Bone-grafting and bone-graft substitutes. *Journal of Bone & Joint Surgery, 84 A*(3), 454-464.

Fishbane, B. M., & Pond RB, S. (1977). Stainless steel fiber reinforcement of polymethylmethacrylate. *Clinical Orthopaedics and Related Research, (*128), 194-199.

Frankenburg, E. P., Goldstein, S. A., Bauer, T. W., Harris, S. A., & Poser, R. D. (1998). Biomechanical and histological evaluation of a calcium phosphate cement. *Journal of Bone & Joint Surgery, 80 A*(8), 1112-1124.

Fujihara, K., Huang, Z. M., Ramakrishna, S., Satknanantham, K., & Hamada, H. (2004). Feasibility of knitted carbon/PEEK composites for orthopedic bone plates. *Biomaterials, 25*(17), 3877-3885.

Gasser, B. (2000). About composite materials and their use in bone surgery. *Injury, 31*(Suppl 4), 48-53.

Giannoudis, P. V., Dinopoulos, H., & Tsiridis, E. (2005). Bone substitutes: An update. *Injury, 36*(Suppl 3), S20-7.

Hacking, S. A., Harvey, E. J., Tanzer, M., Krygier, J. J., & Bobyn, J. D. (2003). Acid-etched microtexture for enhancement of bone growth into porous-coated implants. *The Journal of Bone and Joint Surgery, 85 B*(8), 1182-1189.

Hallan, G., Lie, S. A., Furnes, O., Engesaeter, L. B., Vollset, S. E., & Havelin, L. I. (2007). Medium- and long-term performance of 11,516 uncemented primary femoral stems from the norwegian arthroplasty register. *Journal of Bone & Joint Surgery, 89 B*(12), 1574-1580.

Harris Bryan. (1999). In Harris Bryan (Ed.), *Engineering composite materials* (2nd ed.). London: Institute of Materials, Minerals and Mining.

Heaney, R. P. (2006). Bone biology in health and disease. In M. E. Shils, M. Shike, A. C. Ross, B. Caballero & R. J. Cousins (Eds.), *Modern nutrition in health and disease* (10th Edition ed., pp. 1316-- 1324). 530 Walnut Street, Philadelphia, PA 19106 USA: Lippincott Williams & Wilkins.

Hench, L. L. (1998). Bioactive materials: The potential for tissue regeneration. *Journal of Biomedical Materials Research, 41*(4), 511-518.

Hesse, E., Kluge, G., Atfi, A., Correa, D., Haasper, C., Berding, G., et al. (2010). Repair of a segmental long bone defect in human by implantation of a novel multiple disc graft. *Bone, 46*(5), 1457-1463.

Hildebrand, J., & Scott, R. L. (1950). In Hildebrand J., Scott R. (Eds.), *The solubility of nonelectrolytes* (third ed ed.). New York: Reinhold.

Hornicek, F. J., Gebhardt, M. C., Tomford, W. W., Sorger, J. I., Zavatta, M., Menzner, J. P., et al. (2001). Factors affecting nonunion of the allograft-host junction. *Clinical Orthopaedics & Related Research,* (382), 87-98.

Huiskes, R., Weinans, H., & van Rietbergen, B. (1992). The relationship between stress shielding and bone resorption around total hip stems and the effects of flexible materials. *Clinical Orthopaedics & Related Research,* (274), 124-134.

Ignatius, A. A., Betz, O., Augat, P., & Claes, L. E. (2001). In vivo investigations on composites made of resorbable ceramics and poly(lactide) used as bone graft substitutes. *Journal of Biomedical Materials Research, 58*(6), 701-709.

Itala, A., Koort, J., Ylanen, H. O., Hupa, M., & Aro, H. T. (2003). Biologic significance of surface microroughing in bone incorporation of porous bioactive glass implants. *Journal of Biomedical Materials Research. Part A, 67*(2), 496-503.

Itala, A., Ylanen, H. O., Yrjans, J., Heino, T., Hentunen, T., Hupa, M., et al. (2002). Characterization of microrough bioactive glass surface: Surface reactions and osteoblast responses in vitro. *Journal of Biomedical Materials Research, 62*(3), 404-411.

Itala, A. I., Ylanen, H. O., Ekholm, C., Karlsson, K. H., & Aro, H. T. (2001). Pore diameter of more than 100 microm is not requisite for bone ingrowth in rabbits. *Journal of Biomedical Materials Research, 58*(6), 679-683.

Kane, R. J., Yue, W., Mason, J. J., & Roeder, R. K. (2010). Improved fatigue life of acrylic bone cements reinforced with zirconia fibers. *Journal of the Mechanical Behavior of Biomedical Materials, 3*(7), 504-511.

Karaoglu, S., Baktir, A., Kabak, S., & Arasi, H. (2002). Experimental repair of segmental bone defects in rabbits by demineralized allograft covered by free autogenous periosteum. *Injury, 33*(8), 679-683.

Katoozian, H., Davy, D. T., Arshi, A., & Saadati, U. (2001). Material optimization of femoral component of total hip prosthesis using fiber reinforced polymeric composites. *Medical Engineering & Physics, 23*(7), 503-509.

Keaveny, T. M., Morgan, E. F., Niebur, G. L., & Yeh, O. C. (2001). Biomechanics of trabecular bone. *Annual Review of Biomedical Engineering, 3*, 307-333.

Kim, D. G., Dong, X. N., Cao, T., Baker, K. C., Shaffer, R. R., Fyhrie, D. P., et al. (2006). Evaluation of filler materials used for uniform load distribution at boundaries during structural biomechanical testing of whole vertebrae. *Journal of Biomechanical Engineering, 128*(1), 161-165.

Kim, S., & Watts, D. C. (2004). The effect of reinforcement with woven E-glass fibers on the impact strength of complete dentures fabricated with high-impact acrylic resin [Abstract]. *The Journal of Prosthetic Dentistry, 91*(3) 274-280.

Kolk, A., Handschel, J., Drescher, W., Rothamel, D., Kloss, F., Blessmann, M., et al. (2012). Current trends and future perspectives of bone substitute materials - from space holders to innovative biomaterials. *Journal of Cranio-Maxillo-Facial Surgery - In Press*

Kotha, S. P., Li, C., McGinn, P., Schmid, S. R., & Mason, J. J. (2006). Improved mechanical properties of acrylic bone cement with short titanium fiber reinforcement. *Journal of Materials Science-Materials in Medicine, 17*(12), 1403-1409.

Kotha, S. P., Li, C., Schmid, S. R., & Mason, J. J. (2004). Fracture toughness of steel-fiber-reinforced bone cement. *Journal of Biomedical Materials Research Part A, 70A*(3), 514-521.

Lewis, G. (1997). Properties of acrylic bone cement: State of the art review. *Journal of Biomedical Materials Research, 38*(2), 155-182.

Lieberman, I. H., Togawa, D., & Kayanja, M. M. (2005). Vertebroplasty and kyphoplasty: Filler materials. *The Spine Journal, 5*(6, Supplement), S305-S316.

Lindahl, H., Malchau, H., Herberts, P., & Garellick, G. (2005). Periprosthetic femoral fractures classification and demographics of 1049 periprosthetic femoral fractures from the swedish national hip arthroplasty register. *Journal of Arthroplasty, 20*(7), 857-865.

Livingston, T., Ducheyne, P., & Garino, J. (2002). In vivo evaluation of a bioactive scaffold for bone tissue engineering. *Journal of Biomedical Materials Research, 62*(1), 1-13.

Lotz, J. C., Gerhart, T. N., & Hayes, W. C. (1991). Mechanical properties of metaphyseal bone in the proximal femur. *Journal of Biomechanics, 24*(5), 317-329.

Lu, H. H., Tang, A., Oh, S. C., Spalazzi, J. P., & Dionisio, K. (2005). Compositional effects on the formation of a calcium phosphate layer and the response of osteoblast-like cells on polymer-bioactive glass composites.

Biomaterials, 26(32), 6323-6334.

Lu, J. X., Huang, Z. W., Tropiano, P., Clouet D'Orval, B., Remusat, M., Dejou, J., et al. (2002). Human biological reactions at the interface between bone tissue and polymethylmethacrylate cement. *Journal of Materials Science- Materials in Medicine, 13*(8), 803-809.

Lu, W. W., Cheung, K. M., Li, Y. W., Luk, K. D., Holmes, A. D., Zhu, Q. A., et al. (2001). Bioactive bone cement as a principal fixture for spinal burst fracture: An in vitro biomechanical and morphologic study. *Spine, 26*(24), 2684-2690.

Lucksanasombool, P., Higgs, W. A., Higgs, R. J., Swain, M. V., & Howlett, C. R. (2002). Effects of glass ionomer cements on bone tissue. *Journal of Materials Science-Materials in Medicine, 13*(2), 203-210.

Madison, M., & Martin, R. B. (2001). Repair of fractures with bone defects -FRACTURE HEALING. In M. W. Chapman (Ed.), *Chapman's orthopaedic surgery* (3rd ed., pp. 220--229). 530 Walnut Street, Philadelphia, PA 19106 USA: Lippincott Williams & Wilkins.

Marrs, B., Andrews, R., Rantell, T., & Pienkowski, D. (2006). Augmentation of acrylic bone cement with multiwall carbon nanotubes. *Journal of Biomedical Materials Research Part A, 77 A*(2), 269-276.

Matinlinna, J. P., Lassila, L. V., Ozcan, M., Yli-Urpo, A., & Vallittu, P. K. (2004). An introduction to silanes and their clinical applications in dentistry. *International Journal of Prosthodontics, 17*(2), 155-164.

Mattila R. (2009). Non-resorbable glass fibre-reinforced composite with porous surface as bone substitute material: Experimental studies in vitro and in vivo focused on bone-implant interface. University of Turku.

Mattila, K. T., Heikkila, J. T., Aho, A. J., Manner, I. K., & Dean, P. B. (1995). Massive osteoarticular knee allografts: Structural changes evaluated with CT. *Radiology, 196*(3), 657-660.

Mattila, R. H. (2006). Fibre-reinforced composite implant: In vitro mechanical interlocking with bone model material and residual monomer analysis. *Journal of Materials Science, 41*(13), 4321.

Mattila, R. H., Laurila, P., Rekola, J., Gunn, J., Lassila, L. V. J., Mäntylä, T., et al. (2009). Bone attachment to glass-fibre-reinforced composite implant with porous surface. *Acta Biomaterialia, 5*(5), 1639-1646.

Mattila, R. H., Lassila, L. V. J., & Vallittu, P. K. (2004). Production and structural characterisation of porous fibre-reinforced composite. *Composites Part A: Applied Science and Manufacturing, 35*(6), 631-636.

Mekhail, A. O., & Abraham, Edward Gruber,Brian Gonzalez, Mark. (2004). Bone transport in the management of posttraumatic bone defects in the lower extremity. *Journal of Trauma-Injury Infection & Critical Care, 56*(2), 368-378.

Miettinen, V. M., & Vallittu, P. K. (1997). Release of residual methyl methacrylate into water from glass fibre-poly(methyl methacrylate) composite used in dentures. *Biomaterials, 18*(2), 181-185.

Miller-Chou, B. A., & Koenig, J. L. (2003). A review of polymer dissolution. *Progress in Polymer Science, 28*(8), 1223-1270.

Mittermayer, F., Windhager, R., Dominkus, M., Krepler, P., Schwameis, E., Sluga, M., et al. (2002). Revision of the kotz type of tumour endoprosthesis for the lower limb. *Journal of Bone & Joint Surgery, 84 B*(3), 401-406.

Miyazaki, T., Ohtsuki, C., Kyomoto, M., Tanihara, M., Mori, A., & Kuramoto, K. (2003). Bioactive

PMMA bone cement prepared by modification with methacryloxypropyltrimethoxysilane and calcium chloride. *Journal of Biomedical Materials Research. Part A, 67*(4), 1417-1423.

Moore, W. R., Graves, S. E., & Bain, G. I. (2001). Synthetic bone graft substitutes. *ANZ Journal of Surgery, 71*(6), 354-361.

Morgan, E. F., & Keaveny, T. M. (2001). Dependence of yield strain of human trabecular bone on anatomic site. *Journal of Biomechanics, 34*(5), 569-577.

Murakami, N., Saito, N., Horiuchi, H., Okada, T., Nozaki, K., & Takaoka, K. (2002). Repair of segmental defects in rabbit humeri with titanium fiber mesh cylinders containing recombinant human bone morphogenetic protein-2 (rhBMP-2) and a synthetic polymer. *Journal of Biomedical Materials Research, 62*(2), 169-174.

Narhi, T. O., Jansen, J. A., Jaakkola, T., de Ruijter, A., Rich, J., Seppala, J., et al. (2003). Bone response to degradable thermoplastic composite in rabbits. *Biomaterials, 24*(10), 1697-1704.

Narva, K. K., Lassila, L. V., & Vallittu, P. K. (2005). The static strength and modulus of fiber reinforced denture base polymer. *Dental Materials, 21*(5), 421-428.

Nganga, S., Ylä-Soininmäki, A., Lassila, L. V. J., & Vallittu, P. K. (2011). Interface shear strength and fracture behaviour of porous glass-fibre-reinforced composite implant and bone model material. *Journal of the Mechanical Behavior of Biomedical Materials, 4*(8), 1797-1804.

Nien, Y., Kalidindi, S. R., & Siegler, S. (2001). Fixation strength of swellable bone anchors in low-density polyurethane foam. *Journal of Biomedical Materials Research, 58*(2), 137-146.

Niinomi, M. (2008). Mechanical biocompatibilities of titanium alloys for biomedical applications. *Journal of the Mechanical Behavior of Biomedical Materials, 1*(1), 30-42.

Nishida, J., & Shimamura, T. (2008). Methods of reconstruction for bone defect after tumor excision: A review of alternatives. *Medical Science Monitor, 14*(8), RA107-13.

Oest, M. E., Dupont, K. M., Kong, H. J., Mooney, D. J., & Guldberg, R. E. (2007). Quantitative assessment of scaffold and growth factor-mediated repair of critically sized bone defects. *Journal of Orthopaedic Research, 25*(7), 941-950.

Ohsawa, K., Neo, M., Matsuoka, H., Akiyama, H., Ito, H., & Nakamura, T. (2001). Tissue responses around polymethylmethacrylate particles implanted into bone: Analysis of expression of bone matrix protein mRNAs by in situ hybridization. *Journal of Biomedical Materials Research, 54*(4), 501-508.

Okada, Y., Suka, T., Sim, F. H., Gorski, J. P., & Chao, E. Y. (1988). Comparison of replacement prostheses for segmental defects of bone. different porous coatings for extracortical fixation. *Journal of Bone & Joint Surgery, 70 A*(2), 160-172.

Oonishi, H., Akiyama, H., Takemoto, M., Kawai, T., Yamamoto, K., Yamamuro, T., et al. (2011). The long-term in vivo behavior of polymethyl methacrylate bone cement in total hip arthroplasty. *Acta Orthop, 82*(5), 553-558.

Paley, D., & Maar, D. C. (2000). Ilizarov bone transport treatment for tibial defects. *Journal of Orthopaedic Trauma, 14*(2), 76-85.

Palin, W. M., Fleming, G. J. P., Trevor Burke, F. J., Marquis, P. M., & Randall, R. C. (2003). The reliability in flexural strength testing of a novel dental composite. *Journal of Dentistry, 31*(8), 549-557.

Park, S., & Jin, J. (2001). Effect of silane coupling

agent on interphase and performance of glass Fibers/Unsaturated polyester composites. *Journal of Colloid and Interface Science, 242*(1), 174-179.

Pearson, O. M., & Lieberman, D. E. (2004). The aging of wolff's ?law?: Ontogeny and responses to mechanical loading in cortical bone. *American Journal of Physical Anthropology, 125*(S39), 63-99.

Peltola, M. J., Vallittu, P. K., Vuorinen, V., Aho, A. A., Puntala, A., & Aitasalo, K. M. (2012). Novel composite implant in craniofacial bone reconstruction. *European Archives of Oto-Rhino-Laryngology, 269*(2), 623-628.

Puska, M. A., Lassila, L. V., Aho, A. J., Yli-Urpo, A., Vallittu, P. K., & Kangasniemi, I. (2005). Exothermal characteristics and release of residual monomers from fiber-reinforced oligomer-modified acrylic bone cement. *Journal of Biomaterials Applications, 20*(1), 51-64.

Puska, M. A., Narhi, T. O., Aho, A. J., Yli-Urpo, A., & Vallittu, P. K. (2004). Flexural properties of crosslinked and oligomer-modified glass-fibre reinforced acrylic bone cement. *Journal of Materials Science-Materials in Medicine, 15*(9), 1037-1043.

Puska, M., Yli-Urpo, A., Vallittu, P., & Airola, K. (2005). Synthesis and characterization of polyamide of trans-4-hydroxy-L-proline used as porogen filler in acrylic bone cement. *Journal of Biomaterials Applications, 19*(4), 287-301.

Ramakrishna, S., Mayer, J., Wintermantel, E., & Leong, K. W. (2001). Biomedical applications of polymer-composite materials: A review. *Composites Science and Technology, 61*(9), 1189-1224.

Ramos, V.,Jr, Runyan, D. A., & Christensen, L. C. (1996). The effect of plasma-treated polyethylene fiber on the fracture strength of polymethyl methacrylate. *Journal of Prosthetic Dentistry, 76*(1), 94-96.

Ray, C. D. (1997). Threaded titanium cages for lumbar interbody fusions. *Spine, 22*(6), 667-679.

Reichert, J. C., Saifzadeh, S., Wullschleger, M. E., Epari, D. R., Schutz, M. A., Duda, G. N., et al. (2009). The challenge of establishing preclinical models for segmental bone defect research. *Biomaterials, 30*(12), 2149-2163.

Reilly, G. C., & Currey, J. D. (1999). The development of microcracking and failure in bone depends on the loading mode to which it is adapted. *Journal of Experimental Biology, 202*(5), 543-552.

Revell, P. A., Braden, M., & Freeman, M. A. R. (1998). Review of the biological response to a novel bone cement containing poly(ethyl methacrylate) and n-butyl methacrylate. *Biomaterials, 19*(17), 1579-1586.

Rho, J., Kuhn-Spearing, L., & Zioupos, P. (1998). Mechanical properties and the hierarchical structure of bone. *Medical Engineering & Physics, 20*(2), 92-102.

Rho, J., Tsui, T. Y., & Pharr, G. M. (1997). Elastic properties of human cortical and trabecular lamellar bone measured by nanoindentation. *Biomaterials, 18*(20), 1325-1330.

Ricalde, P., Engroff, S. L., Von Fraunhofer, J. A., & Posnick, J. C. (2005). Strength analysis of titanium and resorbable internal fixation in a mandibulotomy model. *Journal of Oral & Maxillofacial Surgery, 63*(8), 1180-1183.

Saha, S., & Pal, S. (1986). Mechanical characterization of commercially made carbon-fiber-reinforced polymethylmethacrylate. *Journal of Biomedical Materials Research, 20*(6), 817-826.

Saringer, W., Nobauer-Huhmann, I., & Knosp, E. (2002). Cranioplasty with individual carbon fibre reinforced polymere (CFRP) medical

grade implants based on CAD/CAM technique. *Acta Neurochirurgica, 144*(11), 1193-1203.

Sarkar, M. R., Augat, P., Shefelbine, S. J., Schorlemmer, S., Huber-Lang, M., Claes, L., et al. (2006). Bone formation in a long bone defect model using a platelet-rich plasma-loaded collagen scaffold. *Biomaterials, 27*(9), 1817-1823.

Sawyer-Glover, A. M., & Shellock, F. G. (2000). Pre-MRI procedure screening: Recommendations and safety considerations for biomedical implants and devices. *Journal of Magnetic Resonance Imaging, 12*(1), 92-106.

Shapiro, F. (2008). Bone development and its relation to fracture repair. the role of mesenchymal osteoblasts and surface osteoblasts. *European Cells & Materials, 15*, 53-76.

Shellock, F. G. (2002). Biomedical implants and devices: Assessment of magnetic field interactions with a 3.0-tesla MR system. *Journal of Magnetic Resonance Imaging, 16*(6), 721-732.

Shin, D. S., Choong, P. F., Chao, E. Y., & Sim, F. H. (2000). Large tumor endoprostheses and extracortical bone-bridging: 28 patients followed 10-20 years. *Acta Orthopaedica Scandinavica, 71*(3), 305-311.

Stadelmann, V. A., Terrier, A., & Pioletti, D. P. (2008). Microstimulation at the bone-implant interface upregulates osteoclast activation pathways. *Bone, 42*(2), 358-364.

Stipho, H. D. (1998). Effect of glass fiber reinforcement on some mechanical properties of autopolymerizing polymethyl methacrylate. *The Journal of Prosthetic Dentistry, 79*(5), 580-584.

Strandberg, N. Aho, AJ. Tirri, T. Seppälä, J. (2001). Bloaktiivinen lasi metakrylaatti komposiiti kokeellisessa putkiluun segmenttidefektissä. *Suomen Ortopedia Ja Traumatologia, SOT, 24*(5), 613.

Sundfeldt, M., Carlsson ,L.V., Johansson, C.B., Thomsen, P., & Gretzer, C. (2006). Aseptic loosening, not only a question of wear: A review of different theories. *Acta Orthop, 77*(2), 177-197.

Tadic, D., & Epple, M. (2004). A thorough physicochemical characterisation of 14 calcium phosphate-based bone substitution materials in comparison to natural bone. *Biomaterials, 25*(6), 987-994.

Taitsman, J. P., & Saha, S. (1977). Tensile strength of wire-reinforced bone cement and twisted stainless-steel wire. *Journal of Bone & Joint Surgery, 59 A*(3), 419-425.

Tanzer, M., Turcotte, R., Harvey, E., & Bobyn, J. D. (2003). Extracortical bone bridging in tumor endoprostheses. radiographic and histologic analysis. *Journal of Bone & Joint Surgery, 85 A*(12), 2365-2370.

Teixeira, J. O., & Urist, M. R. (1998). Bone morphogenetic protein induced repair of compartmentalized segmental diaphyseal defects. *Archives of Orthopaedic & Trauma Surgery, 117*(1-2), 27-34.

Thomason, J. L., & Porteus, G. (2011). Swelling of glass-fiber reinforced polyamide 66 during conditioning in water, ethylene glycol, and antifreeze mixture. *Polymer Composites, 32*(4), 639-647.

Thompson, R. C.,Jr, Garg, A., Clohisy, D. R., & Cheng, E. Y. (2000). Fractures in large-segment allografts. *Clinical Orthopaedics & Related Research,* (370), 227-235.

Tiemann, A. H., Schmidt, H. G., Braunschweig, R., & Hofmann, G. O. (2009). Strategies for the analysis of osteitic bone defects at the diaphysis of long bones. *Strategies in Trauma & Limb Reconstruction, 4*(1), 13-18.

Tsue, F., Takahashi, Y., & Shimizu, H. (2007). Reinforcing effect of glass-fiber-reinforced composite on flexural strength at the proportional limit of denture base resin. *Acta Odontologica Scandinavica, 65*(3), 141-148.

Turner, C. H. (2006). Bone strength: Current concepts. *Annals of the New York Academy of Sciences, 1068*(1), 429-446.

Tuusa, S. M., Peltola, M. J., Tirri, T., Lassila, L. V., & Vallittu, P. K. (2007). Frontal bone defect repair with experimental glass-fiber-reinforced composite with bioactive glass granule coating. *Journal of Biomedical Materials Research. Part B, Applied Biomaterials, 82*(1), 149-155.

Tuusa, S. M., Peltola, M. J., Tirri, T., Puska, M. A., Roytta, M., Aho, H., et al. (2008). Reconstruction of critical size calvarial bone defects in rabbits with glass-fiber-reinforced composite with bioactive glass granule coating. *Journal of Biomedical Materials Research. Part B, Applied Biomaterials, 84*(2), 510-519.

Valimaki, V. V., & Aro, H. T. (2006). Molecular basis for action of bioactive glasses as bone graft substitute. *Scandinavian Journal of Surgery: SJS, 95*(2), 95-102.

Vallittu, P. K. (1995a). The effect of void space and polymerization time on transverse strength of acrylic-glass fibre composite. *Journal of Oral Rehabilitation, 22*(4), 257-261.

Vallittu, P. K., Vojtkova, H., & Lassila, V. P. (1995b). Impact strength of denture polymethyl methacrylate reinforced with continuous glass fibers or metal wire. *Acta Odontologica Scandinavica, 53*(6), 392-396.

Vallittu, P. K. (1996). A review of fiber-reinforced denture base resins. *Journal of Prosthodontics, 5*(4), 270-276.

Vallittu, P. K. (1997a). Curing of a silane coupling agent and its effect on the transverse strength of autopolymerizing polymethylmethacrylate-glass fibre composite. *Journal of Oral Rehabilitation, 24*(2), 124-130.

Vallittu, P. K. (1997b). Oxygen inhibition of autopolymerization of polymethylmethacrylate-glass fibre composite. *Journal of Materials Science.Materials in Medicine, 8*(8), 489-492.

Vallittu, P. K. (1999). Flexural properties of acrylic resin polymers reinforced with unidirectional and woven glass fibers. *Journal of Prosthetic Dentistry, 81*(3), 318-326.

Vallittu, P. K., & Ekstrand, K. (1999). In vitro cytotoxicity of fibre polymethyl methacrylate composite used in dentures. *Journal of Oral Rehabilitation, 26*(8), 666-671.

Vallittu, P. K. (2001). Strength and interfacial adhesion of FRC tooh system. *The Second International Symposium of Fiber-Reinforced Plastics in Dentistry,* Nijmegen, The Netherland.

Vallittu, P. K. (2007). Effect of 10 years of in vitro aging on the flexural properties of fiber-reinforced resin composites. *International Journal of Prosthodontics, 20*(1), 43-45.

Vallo, C. I., Montemartini, P. E., Fanovich, M. A., Porto Lopez, J. M., & Cuadrado, T. R. (1999). Polymethylmethacrylate-based bone cement modified with hydroxyapatite. *Journal of Biomedical Materials Research, 48*(2), 150-158.

Van Lenthe, G. H., de Waal Malefijt, M. C., & Huiskes, R. (1997). Stress shielding after total knee replacement may cause bone resorption in the distal femur. *Journal of Bone & Joint Surgery, 79 B*(1), 117-122.

Wang, M. (2003). Developing bioactive composite materials for tissue replacement. *Biomaterials, 24*(13), 2133-2151.

Wheeler, D. L., Eschbach, E. J., Hoellrich, R. G.,

Montfort, M. J., & Chamberland, D. L. (2000). Assessment of resorbable bioactive material for grafting of critical-size cancellous defects. *Journal of Orthopaedic Research, 18*(1), 140-148.

Wheeler, D. L., Stokes, K. E., Hoellrich, R. G., Chamberland, D. L., & McLoughlin, S. W. (1998). Effect of bioactive glass particle size on osseous regeneration of cancellous defects. *Journal of Biomedical Materials Research, 41*(4), 527-533.

Wurm, G., Tomancok, B., Holl, K., & Trenkler, J. (2004). Prospective study on cranioplasty with individual carbon fiber reinforced polymer (CFRP) implants produced by means of stereolithography. *Surgical Neurology, 62*(6), 510-521.

Yaszemski, M. J., Payne, R. G., Hayes, W. C., Langer, R., & Mikos, A. G. (1996). Evolution of bone transplantation: Molecular, cellular and tissue strategies to engineer human bone. *Biomaterials, 17*(2), 175-185.

Zhang, C., Wang, J., Feng, H., Lu, B., Song, Z., & Zhang, X. (2001). Replacement of segmental bone defects using porous bioceramic cylinders: A biomechanical and X-ray diffraction study. *Journal of Biomedical Materials Research, 54*(3), 407-411.

Zimmermann, G., & Moghaddam, A. (2011). Allograft bone matrix versus synthetic bone graft substitutes. *Injury, 42*(Suppl 2), S16-21.